Nationwide increase of polycyclic aromatic hydrocarbons in ultrafine particles during winter over China revealed by size-segregated measurements

Qingqing Yu[a], Xiang Ding[a,d,*], Quanfu He[a], Weiqiang Yang[e], Ming Zhu[a,b], Sheng Li[a,b], Runqi Zhang[a,b], Ruqin Shen[a], Yanli Zhang[a,c,d], Xinhui Bi [a,d], Yuesi Wang[c,f], Ping'an Peng[a,d], Xinming Wang[a,b,c,d,*]

[a]State Key Laboratory of Organic Geochemistry and Guangdong Key Laboratory of Environmental Protection and Resources Utilization, Guangzhou Institute of Geochemistry, Chinese Academy of Sciences, Guangzhou 510640, China

[b]University of Chinese Academy of Sciences, Beijing 100049, China

[c]Center for Excellence in Regional Atmospheric Environment, Institute of Urban Environment, Chinese Academy of Sciences, Xiamen 361021, China

[d]Guangdong-Hong Kong-Macao Joint Laboratory for Environmental Pollution and Control, Guangzhou Institute of Geochemistry, Chinese Academy of Science, Guangzhou 510640, China

[e]Guangdong Provincial Academy of Environmental Science, Guangzhou 510045, China

[f]State Key Laboratory of Atmospheric Boundary Layer Physics and Atmospheric Chemistry, Institute of Atmospheric Physics, Chinese Academy of Sciences, Beijing 100029, China

*corresponding author:

Dr. Xinming Wang and Dr. Xiang Ding

State Key Laboratory of Organic Geochemistry Guangzhou Institute of Geochemistry, Chinese Academy of Sciences, 511 Kehua Rd, Tianhe, Guangzhou, 510640, China.

Email addresses: wangxm@gig.ac.cn and xiangd@gig.ac.cn

Abstract

Polycyclic aromatic hydrocarbons (PAHs) are toxic compounds in the atmosphere and have adverse effects on public health, especially through the inhalation of particulate matter (PM). At present, there are limited understandings in size distribution of particulate-bound PAHs and its health risk on a continental scale. In this study, we carried out simultaneously PM campaign from October, 2012 to September, 2013 at 12 sampling sites including urban, sub-urban and remote sites in different regions of China. Size-segregated PAHs and typical tracer of coal combustion (picene), biomass burning (levoglucosan) and vehicle exhaust (hopanes) were measured. The annual averages of total 24 PAHs ($\sum_{24}$PAHs) and benzo[a]pyrene (BaP) carcinogenic equivalent concentration (BaP_{eq}) ranged from 7.56 to 205 ng m^{-3} with a mean of 53.5 ng m^{-3} and 0.21 to 22.2 ng m^{-3} with a mean of 5.02 ng m^{-3}, respectively. At all the sites, $\sum_{24}$PAHs and BaP_{eq} were dominated in the ultrafine particles with aerodynamic diameter <1.1 μm, followed by those in the size ranges of 1.1-3.3 μm and >3.3 μm. Compared with the southern China, the northern China witnessed much higher $\sum_{24}$PAHs (87.36 ng m^{-3} vs. 17.56 ng m^{-3}), BaP_{eq} (8.48 ng m^{-3} vs. 1.34 ng m^{-3}) and PAHs inhalation cancer risk (7.4×10^{-4} vs. 1.2×10^{-4}). Nationwide increases in both PAH levels and inhalation cancer risk occurred in winter. The unfavorable meteorological conditions and enhanced emissions of coal combustion and biomass burning together led to severe PAHs pollution and high cancer risk in the atmosphere of the northern China, especially during winter. Coal combustion is the major source of BaP_{eq} in all size particles at most sampling sites. Our results suggested that the reduction of coal and biofuel consumption in the residential sector could be crucial and effective to lower PAH concentrations and its inhalation cancer risk in China.

Key words: Polycyclic aromatic hydrocarbons; China; inhalation cancer risk; coal combustion; biomass burning

1. Introduction

Ambient particulate matter (PM) pollution has adverse effects on public health. The global deaths caused by exposure to the PM with aerodynamic diameters less than 2.5 μm ($PM_{2.5}$) kept increasing from 1990 and reached 4.2 million in 2015 (Cohen et al., 2017). In China, ambient $PM_{2.5}$ pollution ranked the fourth leading risks for deaths (Yang et al., 2013), and caused 1.7 million premature deaths in 2015 (Song et al., 2017). Adverse health impacts of PM are associated with particle size and chemical components (Chung et al., 2015; Dong et al., 2018). Higher risk of cardiovascular disease was associated with smaller size-fractioned particulate matter, especially $PM_{1.0}$-bound particulate matter (Yin et al., 2020).

Polycyclic aromatic hydrocarbons (PAHs) are a group of organic substances composed of two or more aromatic rings. Due to the mutagenic, teratogenic, and carcinogenic properties (Kim et al., 2013), PAHs are one of the most toxic components in PM (Xu et al., 2008). Toxic PAHs usually enrich in fine particles, especially the aerodynamic diameters less than 1.0 μm (Wang et al., 2016; Li et al., 2019) which can enter the human respiratory system through inhalation (Yu et al., 2015). Exposure to PAHs likely induces DNA damage and raises the risk of gene mutation (Zhang et al., 2012; Lv et al., 2016) and cardiopulmonary mortality (Kuo et al., 2003; John et al., 2009). Previous studies have demonstrated that inhalation exposure to PAHs can cause high risk of lung cancer (Armstrong et al., 2004; Zhang et al., 2009; Shrivastava et al., 2017).

Atmospheric PAHs are mainly emitted from incomplete combustion of fossil fuels and biomasses (Mastral and Callen, 2000). As typical semi-volatile chemicals, PAHs can transport over long distances (Zelenyuk et al., 2012) and have been detected in the global atmosphere

(Brown et al., 2013; Garrido et al., 2014; Hong et al., 2016; Liu et al., 2017a; Hayakawa et al., 2018). Emission inventory indicated that developing countries were the major contributors to global PAHs emission (Zhang and Tao, 2009; Shen et al., 2013a).

As the largest developing country in the world, China has large amounts of PAHs emission and high cancer risk caused by PAHs exposure. The annual emission of 16 USEPA priority PAHs in China sharply increased from 18 Gg in 1980 to 106 Gg in 2007 (Xu et al., 2006; Shen et al., 2013a). China became the largest emitter of PAHs, accounting for about 20% of the global PAHs emission during 2007 (Shen et al., 2013a). The excess lung cancer risk caused by inhalation exposure to ambient PAHs was estimated to be 6.5×10^{-6} in China (Zhang et al., 2009), which was 5.5 times higher than the acceptable risk level of 1.0×10^{-6} in US (USEPA, 1991). As Hong et al. (2016) estimated, the lifetime excess lung cancer cases caused by exposure to PAHs for China ranged from 27.8-2200 per million people and were higher than other Asia counties.

Moreover, PAHs emission and cancer risk in China have large spatial and seasonal variations. As reported by Tao and coworkers, high emission of PAHs occurred in the North China Plain (Zhang et al., 2007), and the emission in winter was 1.6 times higher than that in summer (Zhang and Tao, 2008). Thus, the lung cancer risk caused by ambient PAH inhalation exposure in the northern China was higher than that in the southern China (Zhang et al. 2009). In addition, through long-range atmospheric transport, PAHs emitted in China could spread to other regions of the world (Zhang et al., 2011; Inomata et al., 2012).

For more accurate estimation of inhalation exposure to ambient PAHs and its cancer risks in China, it is essential to carry out nationwide campaigns to acquire spatial and seasonal characteristics of atmospheric PAHs. The data of PAHs in the ambient air are accumulating in

China during the past decades. Among these filed studies, most were conducted in rapidly developing economic regions, including the North China region (Huang et al., 2006; Liu et al., 2007a; Wang et al., 2011; Lin et al., 2015a; Lin et al., 2015b; Tang et al., 2017; Yu et al., 2018), Yangtze River Delta region (Liu et al., 2001; Zhu et al., 2009; Gu et al., 2010; He et al., 2014) and Pearl River Delta region (Bi et al., 2003; Guo et al., 2003; Li et al., 2006; Tan et al., 2006; Duan et al., 2007; Lang et al., 2007; Yang et al., 2010; Gao et al., 2011, 2012, 2013, 2015; Yu et al., 2016), due to large amounts of combustion emission and high density of population in these regions. These studies provided insight into the fate and health risk of airborne PAHs on a local or regional scale. However, due to the inconsistency in sampling methods, frequency and duration in these local and regional campaigns, it is difficult to draw a national picture of PAHs pollution in the air of China.

There are rare dataset discovering nationwide characteristics of airborne PAHs over China. Liu et al. (2007b) reported PAHs in the air of 37 cities across China using passive polyurethane foam (PUF) disks. Wang et al. (2006) and Liu et al., (2017b) determined $PM_{2.5}$-bound PAHs over 14 and 9 Chinese cities, respectively. PAHs in the total suspended particle (TSP) and gas phase were measured over 11 cities in China (Ma et al., 2018; Ma et al., 2020). Besides these important information of PAHs in the bulk PM, it is vital to determine size distribution of PAHs, since the size of particles is directly linked to their potential for causing health problems. On the national scale, at present, there is only one field study available reporting size-segregated atmospheric PAHs at 10 sites (Shen et al., 2019). Therefore, it is essential to carry out large range campaigns coving multiple types of sites across different regions to investigate size distribution of PAHs levels and sources and discover their difference in health risks among

typical regions of China (e.g. north vs. south, urban vs. remote). In this study, we simultaneously collected filter-based size-fractionated PM samples consecutively at 12 sites for one year. We analyzed chemical compositions of PAHs as well as other organic tracers to characterize the spatiotemporal pattern and size distribution of PAHs over China and to explore the possible sources of PAHs on the national scale. This information is helpful to provide a basis for PAHs pollution control and health effects reduction in different regions of China.

2. Materials and Methods

2.1 Field sampling

The PM samples were collected simultaneously at 12 sampling sites across 6 regions of China, containing five urban sites, three sub-urban sites and four remote sites (Figure S1 and Table S1 in the supporting information). The Huai River-Qin Mountains Line is the geographical line that divides China into the northern and southern regions. There are central heating systems in winter in some urban areas of the northern China, but not so in the southern China. The 12 sampling sites are Beijing (BJ), Dunhuang (DH), Hefei (HF), Hailun (HL), Kunming (KM), Qianyanzhou (QYZ), Sanya (SY), Shapotou (SPT), Taiyuan (TY), Tongyu (TYU), Wuxi (WX) and Xishuangbanna (BN). According to their locations, 6 of the 12 sites are situated in the northern China, including BJ, DH, HL, SPT, TY and TYU. And the remaining 6 sites are located in the southern China, including BN, HF, KM, QYZ, SY and WX.

Total suspended particles (TSP) were collected using Anderson 9-stage cascade impactors (<0.4, 0.4-0.7, 0.7-1.1, 1.1-2.1, 2.1-3.3, 3.3-4.7, 4.7-5.8, 5.8-9.0, >9.0 μm) at a constant flow of 28.3 L/min. Quartz fiber filters (Whatman, QMA) that were used to collect PM samples were prebaked for 8 h at 450 ℃. At each site, one set of nine size-fractionated PM samples were

collected for 48-hr every 2 weeks. 294 sets of field samples and one set of field blanks were collected. Detailed information of the field sampling can be found elsewhere (Ding et al., 2014). According to the meteorological definition, each season lasts three months that spring runs from March to May, summer runs from June to August, fall (autumn) runs from September to November, and winter runs from December to February.

The data of average temperature (T), relative humidity (RH), the maximum solar radiation (SR) during each sampling episode were available in the China Meteorological Data Service Center (http://data.cma.cn/en). And the average boundary layer height (BLH) was calculated using the NOAA's READY Archived Meteorology online calculating program (http://ready.arl.noaa.gov/READYamet.php).

2.2 Chemical analysis

Each set of nine filters were combined into three samples with the aerodynamic diameters smaller than 1.1 μm ($PM_{1.1}$), between 1.1 μm and 3.3 μm ($PM_{1.1\text{-}3.3}$), and large than 3.3 μm ($PM_{>3.3}$), respectively. Before ultrasonic solvent extraction, 400 ul of isotope-labeled mixture compounds (tetracosane-d_{50}, napthalene-d_8, acenaphthene-d_{10}, phenethrene-d_{10}, chrysene-d_{12}, perylene-d_{12} and levoglucosan-$^{13}C_6$) were spiked into the samples as internal standards. Samples were ultrasonic extracted twice with the mixed solvent of dichloride methane / hexane (1:1, v/v), and then twice with the mixed solvent of dichloride methane / methanol (1:1, v/v). The extracts of each sample were filtered, combined, and finally concentrated to about 1 mL. Then the extracts were divided into two aliquots for silylation and methylation, respectively. Detailed information about the procedures of silylation and methylation were introduced elsewhere (Ding et al., 2014; Yu et al., 2016).

158 The methylated aliquot was analyzed for PAHs and hopanes using a 7890/5975C gas
159 chromatography/mass spectrometer detector (GC/MSD) in the selected ion monitoring (SIM)
160 mode with a 60 m HP-5MS capillary column (0.25 mm, 0.25 μm). The GC temperature was
161 initiated at 65 ℃, held for 2 min, and then increased to 300 ℃ at 5 ℃ min^{-1} and held for 40
162 min. The silylated aliquot was analyzed for levoglucosan using the same GC/MSD in the scan
163 mode with a 30 m HP-5MS capillary column (0.25 mm, 0.25 μm). The GC temperature was
164 initiated at 65 ℃, held for 2 min, and then increased to 290 ℃ at 5 ℃ min^{-1} and held for 20
165 min. The target compounds were identified by authentic standards and quantified using an
166 internal calibration approach. Table S2 lists the 24 target PAHs and their abbreviations.
167 2.3 Quality control and quality assurance
168 Field and laboratory blanks were analyzed in the same manner as the PM samples. The
169 target compounds were not detected or negligible in the blanks. The data reported in this study
170 were corrected by corresponding field blanks. To test the recovery of the analytical procedure,
171 we analyzed the NIST urban dust Standard Reference Material (SRM 1649b, n=6) in the same
172 manner as the PM samples. Compared with the certified values for PAHs in SRM 1649b, the
173 recoveries were 81.5±1.9%, 66.6±5.4%, 113.6±4.4%, 76.2±2.5%, 100.4±7.9%, 138.3±3.6%,
174 109.5±14.2%, 125.8±8.8% and 86.4±10.7% for Pyr, Ret, Chr, BbF, BkF, BeP, Per, IcdP and Pic
175 respectively. The data reported in this study were not recovery corrected. The method detection
176 limits (MDLs) of the target compounds ranged from 0.01 to 0.08 ng m^{-3}.
177 2.4 Positive matrix factorization (PMF) analysis
178 Positive matrix factorization (PMF) (USEPA, version PMF 5.0) was employed for source
179 apportionment of PAHs. The model has been widely used to attribute major sources of PAHs

(Larsen and Baker, 2003; Belis et al., 2011). In case the observed concentration (*Con*) of a compound was below its MDL, half of the MDL was used as the model input data and the uncertainty (*Unc*) was set as 5/6 of the MDL (Polissar et al., 1998). If the *Con* of a compound was higher than its MDL, *Unc* was calculated as $Unc = [(20\% \times Con)^2 + (MDL)^2]^{1/2}$ (Polissar et al., 1998).

2.5 Exposure assessment

Besides BaP, other PAHs like BaA, BbF, DahA and IcdP are also carcinogenic compounds (IARC, 2001). In order to assess the carcinogenicity of bulk PAHs, the BaP carcinogenic equivalent concentration (BaP_{eq}) was calculated by multiplying the concentrations of PAH individuals (PAH_i) with their toxic equivalency factor (TEF_i) as:

$$BaP_{eq} = \sum_{i=1}^{n} PAH_i \times TEF_i \quad (1)$$

In this study, we adopted the TEFs reported by Nisbet and Lagoy (1992) which were 0.001 for Phe, Flu and Pyr, 0.01 for Ant, Chr and BghiP, 0.1 for BaA, BbF, BkF, BeP, and IcdP, and 1.0 for BaP and DahA. Table S3 lists annual averages of PAH individuals and BaP_{eq} at the 12 sites.

Incremental lifetime lung cancer risk (ILCR) caused by inhalation exposure to PAHs was estimated as:

$$ILCR = BaP_{eq} \times UR_{BaP} \quad (2)$$

where UR_{BaP} is the unit relative risk of BaP. Based on the epidemiological data from studies in coke-oven workers, the lung cancer risk of BaP inhalation was estimated to be 8.7×10^{-5} per ng m^{-3} (WHO, 2000). Thus, we used a UR_{BaP} value of 8.7×10^{-5} per ng/m^3 in this study.

3. Results and discussion

3.1 General marks

Annual averages of the total 24 PAHs ($\sum_{24}$PAHs) in TSP (sum of three PM size ranges) ranged from 7.56 to 205 ng m^{-3} (Figure 1a) among the 12 sampling sites with a mean of 53.5 ng m^{-3}. The highest concentration of $\sum_{24}$PAHs was observed at TY and the lowest level occurred at SY (Figure 1a). Compared with the data in other large scale observations (Table 1), atmospheric concentrations of PAHs measured at the 12 sites in this study were comparable with previously reported values in China in 2013-2014 (Liu et al., 2017b; Shen et al., 2019) and U.S. (Liu et al., 2017a), lower than those measured in China in 2003 and 2008-2009 (Wang et al., 2006; Ma et al., 2018), but higher than those over Great Lakes (Sun et al., 2006), Europe (Jaward et al., 2004), Japan (Hayakawa et al., 2018) and some Asian countries (Hong et al., 2016). Figure 1a also presents the compositions of PAHs. Apparently, 4- and 5-rings PAHs were the majority in $\sum_{24}$PAHs with the mass shares of 36.8±5.6% and 31.4±9.6%, respectively, followed by the PAHs with 3-rings (19.2±9.4%), 6-rings (11.3±3.8%), and 7-rings (1.3±0.6%). The concentrations of $\sum_{24}$PAHs at urban sites (82.7 ng m^{-3}) were significant higher ($p<0.05$) than those at sub-urban (48.0 ng m^{-3}) and remote sites (18.0 ng m^{-3}) (Figure S2).

Annual averages of BaP in TSP among the 12 sites were in the range of 0.09 to 11.0 ng m^{-3} with a mean of 2.58 ng m^{-3}. The highest level of atmospheric BaP occurred at TY and the lowest existed at SY. The BaP values at five sites (WX, BJ, HL, DH and TY) exceeded the national standard of annual atmospheric BaP (1.0 ng m^{-1}) by factors of 1.2 to 11.0. For BaP_{eq}, annual averages ranged from 0.21 to 22.2 ng m^{-3} with the predominant contribution from 5-rings PAHs (Figure 1b). ILCR caused by inhalation exposure to PAHs ranged from 1.8×10^{-5} (SY) -1.9×10^{-3} (TY) among the 12 sites in China (Figure S3), which were much higher than the

acceptable risk level of 1.0×10^{-6} in US (USEPA, 1991). All these demonstrated that China faced severe PAHs pollution and high health risk (Zhang et al., 2009; Shrivastava et al., 2017). And BeP_{eq} (Figure S4) and ILCR (Figure S5) were both the highest at urban sites. All these indicated that people in urban regions of China were faced with higher exposure risk of PAHs pollution as compared to those in sub-urban and remote areas. Figure S6 exhibits that 4- and 5-rings PAHs are the majority in $\sum_{24}$PAHs at urban, sub-urban and remote sites, which totally accounted 72.2%, 63.8% and 66.6% of the total amounts in TSP, respectively. The percentage of 5-rings PAHs dominates at urban sites, and 4-rings PAHs makes the largest proportion at sub-urban and remote sites (Figure S6).

3.2 Enrichment of PAHs in $PM_{1.1}$

Figure 2 presents the size distribution of PAHs and BaP_{eq} at the 12 sites in China. Both $\sum_{24}$PAHs and BaP_{eq} were concentrated in $PM_{1.1}$, accounting for 44.6-71.3% and 56.7-79.3% of the total amounts in TSP, respectively. And BaP_{eq} had more enrichment in $PM_{1.1}$ than $\sum_{24}$PAHs. The mass fractions of $\sum_{24}$PAHs and BaP_{eq} in $PM_{1.1\text{-}3.3}$ were 20.6-39.5% and 16.1-38.3%. The coarse particles ($PM_{>3.3}$) had the lowest loadings of $\sum_{24}$PAHs (7.2-23.4%) and BaP_{eq} (3.0-12.9%). Thus, our observations indicated that PAHs in the ultrafine particles ($PM_{1.1}$) contributed most health risk of PAHs in TSP over China. A previous study at three sites in East Asia found that size distribution of PAHs was unimodal and peaked at 0.7-1.1 μm size (Wang et al., 2009). A recent study at 10 sites of China also found that PAHs were concentrated in $PM_{1.1}$ (Shen et al., 2019). Based on the observation at one site in the Fenhe Plain, northern China, Li et al. (2019) pointed out that PAHs in the particles with the aerodynamic diameters <0.95 μm contributed more than 60% to the total cancer risk of PAHs in PM_{10}. All these results

246 demonstrate that high carcinogenicity of PAHs is accompanied with ultrafine particles,
247 probably because small particles are apt to invade the blood vessels and cause DNA damage.
248 Thus, further studies should put more attentions on PAHs pollution in ultrafine particles.

249 Figure S7 and Figure S8 show seasonal variations in size distribution of $\sum_{24}$PAHs and
250 BaP_{eq}, respectively. $\sum_{24}$PAHs and BaP_{eq} were enriched in $PM_{1.1}$ throughout the year at all sites.
251 The mass fractions of $\sum_{24}$PAHs and BaP_{eq} in $PM_{1.1}$ were the highest during fall to winter (up to
252 74.6% and 79.7% at the DH site), and the lowest during summer (down to 39.2% and 50.7% at
253 the BN site). It should be related to the emission sources of PAHs. Atmospheric PAHs are
254 mainly derived from combustion sources. As Shen et al. (2013b) reported, PAHs emitted form
255 biomass burning and coal combustion enriched in ultrafine particles (<1.1 μm). Moreover, coal
256 combustion witnessed more enrichment of PAHs in ultrafine particles than biomass burning.
257 Figure S9 presents monthly variations in size distribution of PAHs with different number of
258 rings. The mass shares of 3-rings PAHs in $PM_{1.1}$ (39.2%), $PM_{1.1\text{-}3.3}$ (32.0%) and $PM_{>3.3}$ (28.9%)
259 were comparable. And the highest loading of 3-rings PAHs in $PM_{1.1}$ was observed in December
260 2012. The mass fractions of 4-ring PAHs in $PM_{1.1}$ were the highest in December 2012 (58.4%)
261 and the lowest in July 2013 (39.5%). The higher molecular weight PAHs (5-7 rings PAHs) were
262 enriched in $PM_{1.1}$ throughout the year.

263 **3.3 High levels of atmospheric PAHs in the northern China**

264 Figure 3 shows the differences of atmospheric PAHs between the northern China (BJ, DH,
265 HL, SPT, TY and TYU) and southern China (BN, HF, KM, QYZ, SY and WX). $\sum_{24}$PAHs in
266 the northern China was higher than that in the southern China by a factor of 5.0 (Figure 3a).
267 The concentrations of PAHs with different ring number were all higher in the northern China

than those in the southern China, especially for the 4-7 rings PAHs. Moreover, BaP, BaP_{eq} and ILCR in the northern China were 5.8, 5.3 and 5.3 times higher than those in the southern China (Figure 3b). The higher concentrations of PAHs in the air of the northern China than the southern China were also reported in previous field studies (Liu et al., 2017b; Ma et al., 2018; Shen et al., 2019). Based on the emission inventories and model results, previous studies predicted that PAHs concentrations, BaP levels and lung cancer risk of exposure to ambient PAHs in the northern China were all higher than those in the southern China (Xu et al., 2006; Zhang et al., 2007; Zhang and Tao, 2009; Zhu et al., 2015). All these indicated much higher PAHs pollution and health risk in the northern China.

The northern-high feature of atmospheric PAHs should be determined by the meteorological conditions and source emissions. Theoretical relationship between meteorological parameters (temperature, solar radiation and boundary layer height) and the concentration of particulate-bound PAHs were discussed, the detail theoretical discussion information can be found in Text S1 in the supporting information. We illustrate that decrease of ambient temperature would result in the increase of individual PAH in the particulate phase assuming a constant total concentration in the air. The decrease of SR can indeed lower concentrations of hydroxyl radical [OH] and accumulate PAHs in the air, resulting in the increase of PAHs concentrations. And low height of boundary layer can inhibit the vertical diffusion of PAHs, which leads to PAHs accumulation and increased concentrations. As Figure 4 showed, PAHs exhibited strong negative correlations with temperature (T), solar radiation (SR) and the boundary layer height (BLH), especially in the northern China. This indicated that the unfavorable meteorological conditions, such as low levels of temperature, solar radiation

and BLH could lead to PAHs accumulation in the air (Sofuoglu et al., 2001; Callén et al., 2014; Lin et al., 2015a; Li et al., 2016a). In fact, annual averages of T, SR and BLH in the northern China were all significant lower than those in the southern China ($p<0.05$, Table S4), which could indeed cause the accumulation of PAHs in the air of the northern China. In addition, low temperature in the northern China would promote the condensation of semi-volatile PAHs on particles (Wang et al., 2011; Ma et al., 2020). At the southern sites, the negative correlations between PAHs and meteorological parameters (SR and BLH) were not as strong as those in the northern sites. This implied that the adverse influence of meteorological conditions on PAHs pollution in the southern China might be less significant than that in the northern China. The annual ambient temperature at the 12 sampling sites was 13.9 ℃, then we choose 13.9 ℃ to divide the one-year data into warm and cold seasons. As Figure S10 showed, at most sites in the northern and southern China, PAHs negatively correlated with temperature (T), boundary layer height (BLH) and solar radiation (SR) in both cold (T < 13.9 ° C) and warm (T > 13.9 ° C) seasons. Thus, coupled with theoretical discussion, we suggested that worsened PAH pollution in winter was partly caused by adverse meteorological conditions.

For PAHs emission, there are apparent differences in sources and strength between the northern and southern regions. For instance, there is central heating during winter in the northern China, but not so in the southern China. The residential heating during cold period in the northern China could consume large amounts of coal and biofuel, and release substantial PAHs into the air (Liu et al., 2008; Xue et al., 2016). Consequently, atmospheric levels of PAHs in the northern China were much higher than those in the southern China. Since central heating systems start heat supply simultaneously within each region in the northern China, atmospheric

PAHs should increase synchronously within the northern regions of China. To check the spatial homogeneity of PAHs on a regional scale, we analyzed the correlation of PAHs between paired sites within each region. As Table 2 exhibited, PAHs varied synchronously and correlated well at the paired sites in the northern China ($p<0.001$). And closer distance between sites, stronger correlations were observed. The spatial synchronized trends of PAHs observed in the northern regions of China probably resulted from the synchronous variation of PAHs emission in the northern China. In the southern China, although the distances between paired sites were closer than those in the northern regions, the correlations between sites within a region was weaker. This indicated that there might be more local emission which sources and strength vary place to place in the southern China.

We applied diagnostic ratios of PAH isomers to identify major sources of atmospheric PAHs. The ratios of IcdP/(IcdP+BghiP) and Flu/(Flu+Pyr) have been widely used to distinguish possible sources of PAHs (Aceves and Grimalt, 1993; Zhang et al., 2005; Ding et al., 2007; Gao et al., 2012; Lin et al., 2015a; Ma et al., 2018). As summarized by Yunker et al. (2002), the petroleum boundary ratios for IcdP/(IcdP+BghiP) and Flu/(Flu+Pyr) are close to 0.20 and 0.40, respectively; for petroleum combustion, the ratios of IcdP/(IcdP+BghiP) and Flu/(Flu+Pyr) range from 0.20 to 0.50 and 0.40 to 0.50, respectively; and the combustions of grass, wood and coal have the ratios higher than 0.50 for both IcdP/(IcdP+BghiP) and Flu/(Flu+Pyr). As Figure 5 showed, the ratios of Flu/(Flu+Pyr) at the 12 sites ranged from 0.49 to 0.76, suggesting that biomass (grass/wood) burning and coal combustion were the major sources. And the ratios of IcdP/(IcdP+BghiP) were in the range of 0.32 to 0.62, indicating that besides biomass and coal combustion, petroleum combustion, especially vehicle exhaust was also an important source of

atmospheric PAHs. Thus, as identified by the diagnostic ratios, biomass burning, coal combustion and petroleum combustion were major sources of atmospheric PAHs over China. This is also confirmed by the significant correlations of $\sum_{24}$ PAHs with the typical tracers of biomass burning (levoglucosan), coal combustion (picene) and vehicle exhaust (hopanes) at most sites (Figure 6). As global emission inventories showed, PAHs in the atmosphere were mainly released from the incomplete combustion processes including coal combustion, biomass burning and vehicle exhaust (Shen et al., 2013a).

To further attribute PAHs sources, we employed the PMF model to quantify source contributions to atmospheric PAHs at the 12 sites in China. Three factors were identified, and the factor profile resolved by PMF were presented in Figure S11. The first factor was identified as biomass burning, as it had high loadings of the biomass burning tracer, levoglucosan and light weight molecular PAHs such as Phe, Ant, Flu and Pyr which are largely emitted from biomass burning (Li et al., 2016b). The second factor was considered to be coal combustion, as it was characterized by high fractions of the coal combustion marker, picene and the high molecular weight PAHs (Shen et al., 2013b). The third factor was regarded as vehicle exhaust, as it was featured by presence of hopanes, which are molecular markers tracking vehicle exhaust (Cass, 1998; Dai et al., 2015). As Figure S12 showed, there was significant agreement between the predicted and measured PAHs at each site (R^2 in the range of 0.78 to 0.99, $p<0.001$). As the emission inventory of PAHs in China showed, residential/commercial, industrial and transportation were the major sectors of atmospheric PAHs in 2013 (Figure S13, http://inventory.pku.edu.cn). Residential/commercial and industrial sectors mainly consumed coal and biofuel while transportation consumed oil (Shen et al., 2013a). Thus, the mainly

356 sources of PAHs in China were coal combustion, biomass burning and petroleum combustion
357 (especially vehicle exhaust).

358 Figure 7a presents atmospheric PAHs emitted from different sources in China. In the
359 northern China, coal combustion was the major source of atmospheric PAHs (73.6 ng m^{-3}, 84.2%
360 of $\sum_{24}$PAHs), followed by biomass burning (11.8 ng m^{-3} and 13.5%) and vehicle exhaust (2.0
361 ng m^{-3} and 2.3%). In the southern China, coal combustion (9.6 ng m^{-3} and 54.8%) and biomass
362 burning (6.8 ng m^{-3} and 39.0%) were the major contributors, followed by vehicle exhaust (1.1
363 ng m^{-3} and 6.2%). Atmospheric PAHs emitted from the three sources in the northern China were
364 all higher than those in the southern China, especially from coal combustion. Thus, coal
365 combustion was the most important source of atmospheric PAHs in China and caused large
366 increases in PAHs pollution in the northern China. As China statistics yearbook recorded
367 (http://www.stats.gov.cn/english/Statisticaldata/AnnualData/), coal was the dominant fuel in
368 China, accounting for 70.6% (24.1×10^8 tons of Standard Coal Equivalent, SCE) of total primary
369 energy consumption in 2012, followed by crude oil 19.9% (6.7×10^8 tons of SCE) and other
370 types of energy 9.5%, including biofuel, natural gas, hydro power, nuclear power and other
371 power (3.2×10^8 tons of SCE). Although the biofuel consumption was lower than crude oil, the
372 poor combustion conditions during residential biofuel burning could led to higher PAHs
373 emissions as compared to petroleum combustion.

374 We further compared our results with those in the PAHs emission inventory of China
375 (http://inventory.pku.edu.cn) (Figure S14). Our source apportionment results focused on fuel
376 types, while the emission inventory classified the sources into 6 socioeconomic sectors
377 (residential & commercial activities, industry, energy production, agriculture, deforestation &

wildfire, and transportation). Since the transportation mainly used liquid petroleum (gasoline and diesel) and the rest sectors mainly consumed solid fuels (coal and biomass), we grouped these sectors into liquid petroleum combustion and solid fuel burning to directly compare with our results. As Figure S14 showed, both our observation and emissions inventory demonstrated that the PAHs contributions from solid fuel burning was higher in the northern China, while the PAHs contributions from liquid petroleum combustion was higher in the southern China.

Atmospheric PAHs emitted from different sources at urban, sub-urban and remote sites (Figure 7b) and different size particles (Figure 7c) were discussed. At urban and sub-urban sites, coal combustion was the largest source of $\sum_{24}$PAHs (70.4 ng m^{-3}, 85.1% and 30.5 ng m^{-3}, 63.5%), followed by biomass burning (10.1 ng m^{-3}, 12.2% and 16.3 ng m^{-3}, 33.9%) and vehicle emission (2.2 ng m^{-3}, 2.6% and 1.2 ng m^{-3}, 2.5%), while at remote sites the contributions of coal combustion (9.1 ng m^{-3}, 50.6%) and biomass burning (7.8 ng m^{-3}, 43.7%) were comparable and vehicle emission (1.0 ng m^{-3}, 5.7%) had minor contributions. The major sources of $\sum_{24}$PAHs varied among different size particles in the northern and southern China (Figure 7c). For $PM_{>3.3}$-bound PAHs, the contributions of coal combustion (50.3%) and biomass burning (48.4%) were comparable in the northern China, while biomass burning (71.0%) was the largest source in the southern China. For $PM_{1.1\text{-}3.3}$-bound PAHs, coal combustion (66.7%) was the dominated source in the northern China, whereas the percentage of biomass burning (53.7%) was larger than that of coal combustion (40.4%) in the southern China. For $PM_{1.1}$-bound PAHs, coal combustion was the dominated source in the northern (66.6%) and southern (59.3%) China.

Source apportionment of BaP_{eq} in different regions (Figure 7d), sampling sites (Figure 7e) and size particles (Figure 7f) were also discussed. Unlike $\sum_{24}$PAHs, coal combustion was the

predominant source of BaP_{eq} in the northern (8.1 ng m^{-3} and 95.7%) and the southern (1.1 ng m^{-3} and 84.7%) China. The contributions of coal contribution at urban sites (8.3 ng m^{-3} and 96.4%) were larger than those at sub-urban (3.3 ng m^{-3} and 90.8%) and remote (1.0 ng m^{-3} and 82.5%) sites. Coal combustion was the dominating source in different size particles. And its contributions to $PM_{>3.3}$, $PM_{1.1\text{-}3.3}$ and $PM_{1.1}$-bound PAHs in the northern China (87.3%, 95.6% and 96.9%) were all larger than those in the southern China (76.8%, 87.3% and 88.2%).

In terms of incremental lifetime lung cancer risk (ILCR) induced by ambient PAHs, coal combustion was the largest source to total ILCR, accounting for 95.7% (7.1×10^{-4}) and 84.7% (1.0×10^{-4}) in the northern and southern China, respectively (Figure S15). The ILCR due to coal combustion was as high as 1.9×10^{-3} at the TY site in Shanxi province, which was three orders of magnitude higher than the acceptable risk level of 1.0×10^{-6} recommended by USEPA (1991). Shanxi province has the largest coal industry in China, including coal mining and coking production. Previous studies have reported that higher lung cancer risks occurred in Shanxi province, largely owing to the extremely high inhalation exposure of PAHs there (Xia et al., 2013; Liu et al., 2017b; Han et al., 2020). It should be noted that although the contributions of biomass burning (2.1%, 1.6×10^{-5} vs. 6.4%, 7.5×10^{-6}) and vehicle emission (2.2%, 1.6×10^{-5} vs. 8.9%, 1.0×10^{-5}) to total ILCR were minor in the northern and southern China, their ILCR were both exceed the acceptable risk level of 1.0×10^{-6} (USEPA, 1991). Thus, the health risks from biomass burning and vehicle emission cannot be ignored.

Figure S16 shows different source contributions to ILCR at the urban, sub-urban and remote sites. Coal combustion was the dominant source to total ILCR, which accounted for 96.4% (7.2×10^{-4}) at the urban sites, 90.8% (2.9×10^{-4}) at the sub-urban sites, and 82.5% ($8.6\times10^{-}$

422 ^{5}) at the remote sites. The ILCR from biomass burning were the highest at the urban sites
423 (1.3×10^{-5}), followed by the sub-urban (1.2×10^{-5}) and remote sites (9.5×10^{-6}). For vehicle
424 emission, the ILCR were 1.4×10^{-5}, 1.7×10^{-5}, and 8.7×10^{-6} at the urban, sub-urban and remote
425 sites. Our results indicated that even the remote areas in China would face high health risks
426 since the ILCR from the least contributor (e.g. 8.7×10^{-6} for vehicle emission) were exceed the
427 acceptable risk level of 1.0×10^{-6} (USEPA, 1991).

428 Here, we concluded that the unfavorable meteorological conditions and intensive emission
429 especially in coal combustion together led to severe PAHs pollution and high cancer risk in the
430 atmosphere of the northern China.

431 **3.4 Nationwide increase of PAHs pollution and health risk during winter**

432 Figure 8 exhibits monthly variations of BaP_{eq} and ILCR at the 12 sites. BaP_{eq} levels were
433 the highest in winter and the lowest in summer at all sites. As Figure 8 showed, the enhancement
434 of BaP_{eq} from summer to winter ranged from 1.05 (SY) to 32.5 (SPT). And such an
435 enhancement was much more significant at the northern sites than the southern sites. Hence,
436 ILCR was significantly enhanced in winter, especially in the northern China (Figure 8) and was
437 much higher than the acceptable risk level of 1.0×10^{-6} in US (USEPA, 1991). Previous studies
438 in different cities of China also reported such a winter-high trend of atmospheric PAHs (Liu et
439 al., 2017b; Ma et al., 2018; Shen et al., 2019). Thus, there is a nationwide increase of PAHs
440 pollution during winter in China.

441 The winter-high feature of PAHs pollution should result from the impacts of
442 meteorological conditions and source emissions. The winter to summer ratios of PAHs
443 correlated well with that for temperature (Figure S17). And T, SR and BLH were all the lowest

during winter and the highest during summer (Table S5-7). Coupled with the negative correlations between PAHs and meteorological factors (Figure 4), the unfavorable meteorological conditions in wintertime did account for the increase in PAHs pollution.

Moreover, PAHs emitted from coal combustion and biomass burning apparently elevated during fall-winter (Figure 9). In the northern China, central heating systems in urban areas usually start from November to next March. Meanwhile residential heating in the rural areas of northern China consumes substantial coal and biofuel (Xue et al., 2016). Thus, the energy consumption in the residential sector is dramatically enhanced during fall-winter (Xue et al., 2016). In the southern China, although there is no central heating system in urban areas, power plant and industry consume large amounts of coal. And there is also residential coal/biofuel consumption for heating during winter as well as cooking in rural areas (Zhang et al., 2013; Xu et al., 2015). In addition, open burning of agriculture residuals which accounts for a major fraction of the total biomass burning in China will significantly increase during fall-winter harvest seasons in the southern China (Zhang et al., 2013). Our observation and emissions inventory witnessed similar monthly trends that the PAHs from solid fuel combustion (coal and biomass) apparently elevated during fall-winter in the northern and southern China (Figure S18). Previous field studies also found that the contributions of coal combustion and biomass burning to PAHs elevated during fall-winter (Lin et al., 2015a; Yu et al., 2016). Thus, we concluded that the unfavorable meteorological conditions and intensive source emission together led to the increase of PAHs pollution during winter.

Figure S19 presents seasonal variation of ILCR from different sources. The ILCR values from three major sources all elevated during winter. Coal combustion was the largest source to

ILCR, accounting for 94.4% (4.2×10^{-4}), 94.1% (10.8×10^{-4}), 89.2% (1.8×10^{-4}) and 83.8% (6.5×10^{-5}) in fall, winter, spring and summer, respectively. The ILCR from biomass burning was highest in winter (3.7×10^{-5}), followed by spring (1.1×10^{-5}), fall (9.1×10^{-6}) and summer (7.9×10^{-6}). For vehicle emission, the ILCR were 1.6×10^{-5}, 3.0×10^{-5}, 1.1×10^{-5} and 4.7×10^{-6} in fall, winter, spring and summer, respectively. Our results revealed that even in summer people would face high health risks since the ILCR from the least contributor (e.g. 4.7×10^{-6} for vehicle emission) was exceed the acceptable risk level of 1.0×10^{-6} (USEPA, 1991).

Data availability

The data are given in the Supplement.

Author contributions

Qingqing Yu analyzed the data, wrote the paper and performed data interpretation. Quanfu He and Ruqin Shen analyzed the samples. Weiqiang Yang ran the PMF model and helped with the interpretation. Ming Zhu, Sheng Li and Runqi Zhang provided the meteorological data and prepared the related interpretation. Yanli Zhang and Xinhui Bi gave many suggestions about the results and discussion. Yuesi Wang helped the field observation and performed data interpretation. Xiang Ding, Ping'an Peng and Xinming Wang performed data interpretation, reviewed and edited this paper.

Competing interests

The authors declare that they have no conflict of interest.

Acknowledgement

This study was funded by the National Natural Science Foundation of China (41530641/4191101024/41722305/41907196), the National Key Research and Development

Program (2016YFC0202204/2018YFC0213902), the Chinese Academy of Sciences (XDA05100104/QYZDJ-SSW-DQC032), and Guangdong Foundation for Science and Technology Research (2019B121205006/2017BT01Z134/ 2020B1212060053).

492 **References**

493 Aceves, M., and Grimalt, J. O.: Seasonally dependent size distributions of aliphatic and
494 polycyclic aromatic hydrocarbons in urban aerosols from densely populated areas,
495 Environ. Sci. Technol., 27, 2896-2908, https://doi.org/10.1021/Es00049a033, 1993.
496 Armstrong, B., Hutchinson, E., Unwin, J., and Fletcher, T.: Lung cancer risk after exposure to
497 polycyclic aromatic hydrocarbons: A review and meta-analysis, Environ. Health. Persp.,
498 112, 970-978, https://doi.org/10.1289/ehp.6895, 2004.
499 Belis, C. A., Cancelinha, J., Duane, M., Forcina, V., Pedroni, V., Passarella, R., Tanet, G.,
500 Douglas, K., Piazzalunga, A., Bolzacchini, E., Sangiorgi, G., Perrone, M. G., Ferrero, L.,
501 Fermo, P., and Larsen, B. R.: Sources for PM air pollution in the Po Plain, Italy: I. Critical
502 comparison of methods for estimating biomass burning contributions to benzo(a)pyrene,
503 Atmos. Environ., 45, 7266-7275, https://doi.org/10.1016/j.atmosenv.2011.08.061, 2011.
504 Bi, X. H., Sheng, G. Y., Peng, P. A., Chen, Y. J., Zhang, Z. Q., and Fu, J. M.: Distribution of
505 particulate- and vapor-phase n-alkanes and polycyclic aromatic hydrocarbons in urban
506 atmosphere of Guangzhou, China, Atmos. Environ., 37, 289-298,
507 https://doi.org/10.1016/S1352-2310(02)00832-4, 2003.
508 Brown, A. S., Brown, R. J. C., Coleman, P. J., Conolly, C., Sweetman, A. J., Jones, K. C.,
509 Butterfield, D. M., Sarantaridis, D., Donovan, B. J., and Roberts, I.: Twenty years of
510 measurement of polycyclic aromatic hydrocarbons (PAHs) in UK ambient air by
511 nationwide air quality networks, Environ. Sci.-Proc. Imp., 15, 1199-1215,
512 https://doi.org/10.1039/c3em00126a, 2013.
513 Callén, M. S., Iturmendi, A., and López, J. M.: Source apportionment of atmospheric $PM_{2.5}$-

514 bound polycyclic aromatic hydrocarbons by a PMF receptor model. Assessment of
515 potential risk for human health, Environ. Pollut., 195, 167-177,
516 http://dx.doi.org/10.1016/j.envpol.2014.08.025, 2014.
517 Cass, G. R.: Organic molecular tracers for particulate air pollution sources, Trac.-Trend Anal.
518 Chem., 17, 356-366, http://dx.doi.org/10.1016/S0165-9936(98)00040-5, 1998.
519 Chung, Y., Dominici, F., Wang, Y., Coull, B. A., and Bell, M. L.: Associations between long-
520 term exposure to chemical constituents of fine particulate matter ($PM_{2.5}$) and mortality in
521 medicare enrollees in the eastern United States, Environ. Health Persp., 123, 467-474,
522 http://dx.doi.org/10.1289/ehp.1307549, 2015.
523 Cohen, A. J., Brauer, M., Burnett, R., Anderson, H. R., Frostad, J., Estep, K., Balakrishnan, K.,
524 Brunekreef, B., Dandona, L., Dandona, R., Feigin, V., Freedman, G., Hubbell, B., Jobling,
525 A., Kan, H., Knibbs, L., Liu, Y., Martin, R., Morawska, L., Pope, C. A., Shin, H., Straif,
526 K., Shaddick, G., Thomas, M., van Dingenen, R., van Donkelaar, A., Vos, T., Murray, C.
527 J. L., and Forouzanfar, M. H.: Estimates and 25-year trends of the global burden of disease
528 attributable to ambient air pollution: An analysis of data from the Global Burden of
529 Diseases Study 2015, Lancet, 389, 1907-1918, http://dx.doi.org/10.1016/S0140-
530 6736(17)30505-6, 2017.
531 Dai, S., Bi, X., Chan, L. Y., He, J., Wang, B., Wang, X., Peng, P., Sheng, G., and Fu, J.: Chemical
532 and stable carbon isotopic composition of $PM_{2.5}$ from on-road vehicle emissions in the
533 PRD region and implications for vehicle emission control policy, Atmos. Chem. Phys., 15,
534 3097-3108, http://dx.doi.org/10.5194/acp-15-3097-2015, 2015.
535 Ding, X., He, Q. F., Shen, R. Q., Yu, Q. Q., and Wang, X. M.: Spatial distributions of secondary

organic aerosols from isoprene, monoterpenes, beta-caryophyllene, and aromatics over China during summer, J. Geophys. Res.-Atmos., 119, 11877-11891, http://dx.doi.org/10.1002/2014JD021748, 2014.

Ding, X., Wang, X. M., Xie, Z. Q., Xiang, C. H., Mai, B. X., Sun, L. G., Zheng, M., Sheng, G. Y., Fu, J. M., and Poschl, U.: Atmospheric polycyclic aromatic hydrocarbons observed over the North Pacific Ocean and the Arctic area: Spatial distribution and source identification, Atmos. Environ., 41, 2061-2072, http://dx.doi.org/10.1016/j.atmonsenv.2006.11.002, 2007.

Dong, W., Pan, L., Li, H., Miller, M. R., Loh, M., Wu, S., Xu, J., Yang, X., Shan, J., Chen, Y., Deng, F., and Guo, X.: Association of size-fractionated indoor particulate matter and black carbon with heart rate variability in healthy elderly women in Beijing, Indoor Air, 28, 373-382, http://dx.doi.org/10.1111/ina.12449, 2018.

Duan, J. C., Bi, X. H., Tan, J. H., Sheng, G. Y., and Fu, J. M.: Seasonal variation on size distribution and concentration of PAHs in Guangzhou city, China, Chemosphere, 67, 614-622, http://dx.doi.org/10.1016/j.chemosphere.2006.08.030, 2007.

Gao, B., Guo, H., Wang, X. M., Zhao, X. Y., Ling, Z. H., Zhang, Z., and Liu, T. Y.: Polycyclic aromatic hydrocarbons in $PM_{2.5}$ in Guangzhou, southern China: Spatiotemporal patterns and emission sources, J. Hazard. Mater., 239, 78-87, http://dx.doi.org/10.1016/j.jhazmat.2012.07.068, 2012.

Gao, B., Guo, H., Wang, X. M., Zhao, X. Y., Ling, Z. H., Zhang, Z., and Liu, T. Y.: Tracer-based source apportionment of polycyclic aromatic hydrocarbons in $PM_{2.5}$ in Guangzhou, southern China, using positive matrix factorization (PMF), Environ. Sci. Pollut. R., 20,

2398-2409, http://dx.doi.org/10.1007/s11356-012-1129-0, 2013.

Gao, B., Wang, X. M., Zhao, X. Y., Ding, X., Fu, X. X., Zhang, Y. L., He, Q. F., Zhang, Z., Liu, T. Y., Huang, Z. Z., Chen, L. G., Peng, Y., and Guo, H.: Source apportionment of atmospheric PAHs and their toxicity using PMF: Impact of gas/particle partitioning, Atmos. Environ., 103, 114-120, http://dx.doi.org/10.1016/j.atmosenv.2014.12.006, 2015.

Gao, B., Yu, J. Z., Li, S. X., Ding, X., He, Q. F., and Wang, X. M.: Roadside and rooftop measurements of polycyclic aromatic hydrocarbons in $PM_{2.5}$ in urban Guangzhou: Evaluation of vehicular and regional combustion source contributions, Atmos. Environ., 45, 7184-7191, http://dx.doi.org/10.1016/j.atmosenv.2011.09.005, 2011.

Garrido, A., Jiménez-Guerrero, P., and Ratola, N.: Levels, trends and health concerns of atmospheric PAHs in Europe, Atmos. Environ., 99, 474-484, http://dx.doi.org/10.1016/j.atmosenv.2014.10.011, 2014.

Gu, Z. P., Feng, J. L., Han, W. L., Li, L., Wu, M. H., Fu, J. M., and Sheng, G. Y.: Diurnal variations of polycyclic aromatic hydrocarbons associated with $PM_{2.5}$ in Shanghai, China, J. Environ. Sci., 22, 389-396, http://dx.doi.org/10.1016/S1001-0742(09)60120-0, 2010.

Guo, H., Lee, S. C., Ho, K. F., Wang, X. M., and Zou, S. C.: Particle-associated polycyclic aromatic hydrocarbons in urban air of Hong Kong, Atmos. Environ., 37, 5307-5317, http://dx.doi.org/10.1016/j.atmosenv.2003.09.011, 2003.

Han, F., Guo, H., Hu, J., Zhang, J., Ying, Q., and Zhang, H.: Sources and health risks of ambient polycyclic aromatic hydrocarbons in China, Sci. Total Environ., 698, 134229, https://doi.org/10.1016/j.scitotenv.2019.134229, 2020.

Hayakawa, K., Tang, N., Nagato, E. G., Toriba, A., Sakai, S., Kano, F., Goto, S., Endo, O.,

Arashidani, K.-i., and Kakimoto, H.: Long term trends in atmospheric concentrations of polycyclic aromatic hydrocarbons and nitropolycyclic aromatic hydrocarbons: A study of Japanese cities from 1997 to 2014, Environ. Pollut., 233, 474-482, https://doi.org/10.1016/j.envpol.2017.10.038, 2018.

He, J. B., Fan, S. X., Meng, Q. Z., Sun, Y., Zhang, J., and Zu, F.: Polycyclic aromatic hydrocarbons (PAHs) associated with fine particulate matters in Nanjing, China: Distributions, sources and meteorological influences, Atmos. Environ., 89, 207-215, http://dx.doi.org/10.1016/j.atmosenv.2014.02.042, 2014.

Hong, W. J., Jia, H. L., Ma, W. L., Sinha, R. K., Moon, H.-B., Nakata, H., Minh, N.H., Chi, K. H., Li, W. L., Kannan, K., Sverko, E., and Li, Y. F.: Distribution, fate, inhalation exposure and lung cancer risk of atmospheric polycyclic aromatic hydrocarbons in some Asian countries, Environ. Sci. Technol., 13, 7163-7174, http://dx.doi.org/10.1021/acs.est.6b01090, 2016.

Huang, X. F., He, L. Y., Hu, M., and Zhang, Y. H.: Annual variation of particulate organic compounds in $PM_{2.5}$ in the urban atmosphere of Beijing, Atmos. Environ., 40, 2449-2458, http://dx.doi.org/10.1016/j.atmosenv.2005.12.039, 2006.

Inomata, Y., Kajino, M., Sato, K., Ohara, T., Kurokawa, J. I., Ueda, H., Tang, N., Hayakawa, K., Ohizumi, T., and Akimoto, H.: Emission and atmospheric transport of particulate PAHs in Northeast Asia, Environ. Sci. Technol., 46, 4941-4949, http://dx.doi.org/10.1021/es300391w, 2012.

International Agency for Research on Cancer, 2001. Overall Evaluations of Carcinogenicity to Humans.

602 Jaward, F. M., Farrar, N. J., Harner, T., Sweetman, A. J., and Jones, K. C.: Passive air sampling
603 of polycyclic aromatic hydrocarbons and polychlorinated naphthalenes across Europe,
604 Environ. Toxicol. Chem., 23, 1355-1364, http://dx.doi.org/10.1897/03-420, 2004.
605 John, K., Ragavan, N., Pratt, M. M., Singh, P. B., Al-Buheissi, S., Matanhelia, S. S., Phillips,
606 D. H., Poirier, M. C., and Martin, F. L.: Quantification of phase I/II metabolizing enzyme
607 gene expression and polycyclic aromatic hydrocarbon–DNA adduct levels in human
608 prostate, The Prostate, 69, 505-519, http://dx.doi.org/10.1002/pros.20898, 2009.
609 Kim, K. H., Jahan, S. A., Kabir, E., and Brown, R. J. C.: A review of airborne polycyclic
610 aromatic hydrocarbons (PAHs) and their human health effects, Environ. Int., 60, 71-80,
611 http://dx.doi.org/10.1016/j.envint.2013.07.019, 2013.
612 Kuo, C. Y., Hsu, Y. W., and Lee, H. S.: Study of human exposure to particulate PAHs using
613 personal air samplers, Arch. Environ. Con. Tox., 44, 0454-0459,
614 http://dx.doi.org/10.1007/s00244-002-1177-4, 2003.
615 Lang, C., Tao, S., Wang, X. J., Zhang, G., Li, J., and Fu, J. M.: Seasonal variation of polycyclic
616 aromatic hydrocarbons (PAHs) in Pearl River Delta region, China, Atmos. Environ., 41,
617 8370-8379, http://dx.doi.org/10.1016/j.atmosenv.2007.06.015, 2007.
618 Larsen, R. K., and Baker, J. E.: Source apportionment of polycyclic aromatic hydrocarbons in
619 the urban atmosphere: A comparison of three methods, Environ. Sci. Technol., 37, 1873-
620 1881, http://dx.doi.org/10.1021/es0206184, 2003.
621 Li, H. Y., Guo, L. L., Cao, R. F., Gao, B., Yan, Y. L., and He, Q. S.: A wintertime study of $PM_{2.5}$-
622 bound polycyclic aromatic hydrocarbons in Taiyuan during 2009-2013: Assessment of
623 pollution control strategy in a typical basin region, Atmos. Environ., 140, 404-414,

http://dx.doi.org/10.1016/j.atmosenv.2016.06.013, 2016a.

Li, H., Li, H., Zhang, L., Cheng, M., Guo, L., He, Q., Wang, X., and Wang, Y.: High cancer risk from inhalation exposure to PAHs in Fenhe Plain in winter: A particulate size distribution-based study, Atmos. Environ., 216, 116924, https://doi.org/10.1016/j.atmosenv.2019.116924, 2019.

Li, J., Zhang, G., Li, X. D., Qi, S. H., Liu, G. Q., and Peng, X. Z.: Source seasonality of polycyclic aromatic hydrocarbons (PAHs) in a subtropical city, Guangzhou, South China, Sci. Total Environ., 355, 145-155, https://doi.org/10.1016/j.scitotenv.2005.02.042, 2006.

Li, X., Yang, Y., Xu, X., Xu, C., and Hong, J.: Air pollution from polycyclic aromatic hydrocarbons generated by human activities and their health effects in China, J. Clean Prod., 112, 1360-1367, http://dx.doi.org/10.1016/j.jclepro.2015.05.077, 2016b.

Lin, Y., Ma, Y. Q., Qiu, X. H., Li, R., Fang, Y. H., Wang, J. X., Zhu, Y. F., and Hu, D.: Sources, transformation, and health implications of PAHs and their nitrated, hydroxylated, and oxygenated derivatives in $PM_{2.5}$ in Beijing, J. Geophys. Res.- Atmos., 120, 7219-7228, http://dx.doi.org/10.1002/2015JD023628, 2015a.

Lin, Y., Qiu, X. H., Ma, Y. Q., Ma, J., Zheng, M., and Shao, M.: Concentrations and spatial distribution of polycyclic aromatic hydrocarbons (PAHs) and nitrated PAHs (NPAHs) in the atmosphere of North China, and the transformation from PAHs to NPAHs, Environ. Pollut., 196, 164-170, http://dx.doi.org/10.1016/j.envpol.2014.10.005, 2015b.

Liu, B., Xue, Z., Zhu, X., and Jia, C.: Long-term trends (1990–2014), health risks, and sources of atmospheric polycyclic aromatic hydrocarbons (PAHs) in the U.S., Environ. Pollut., 220, 1171-1179, http://dx.doi.org/10.1016/j.envpol.2016.11.018, 2017a.

Liu, D., Lin, T., Syed, J. H., Cheng, Z. N., Xu, Y., Li, K. C., Zhang, G., and Li, J.: Concentration, source identification, and exposure risk assessment of $PM_{2.5}$-bound parent PAHs and nitro-PAHs in atmosphere from typical Chinese cities, Sci. Rep.-UK, 7, 10398, http://dx.doi.org/10.1038/s41598-017-10623-4, 2017b.

Liu, S. Z., Tao, S., Liu, W. X., Dou, H., Liu, Y. N., Zhao, J. Y., Little, M. G., Tian, Z. F., Wang, J. F., Wang, L. G., and Gao, Y.: Seasonal and spatial occurrence and distribution of atmospheric polycyclic aromatic hydrocarbons (PAHs) in rural and urban areas of the North Chinese Plain, Environ. Pollut., 156, 651-656, http://dx.doi.org/10.1016/j.envpol.2008.06.029, 2008.

Liu, S. Z., Tao, S., Liu, W. X., Liu, Y. N., Dou, H., Zhao, J. Y., Wang, L. G., Wang, J. F., Tian, Z. F., and Gao, Y.: Atmospheric polycyclic aromatic hydrocarbons in north China: A winter-time study, Environ. Sci. Technol., 41, 8256-8261, http://dx.doi.org/10.1021/es0716249, 2007a.

Liu, X., Zhang, G., Li, J., Cheng, H. R., Qi, S. H., Li, X. D., and Jones, K. C.: Polycyclic aromatic hydrocarbons (PAHs) in the air of Chinese cities, J. Environ. Monitor., 9, 1092-1098, http://dx.doi.org/10.1039/b707977j, 2007b.

Liu, Y. J., Zhu, L. Z., and Shen, X. Y.: Polycyclic aromatic hydrocarbons (PAHs) in indoor and outdoor air of Hangzhou, China, Environ. Sci. Technol., 35, 840-844, http://dx.doi.org/10.1021/es001354t, 2001.

Lv, Y., Li, X., Xu, T. T., Cheng, T. T., Yang, X., Chen, J. M., Iinuma, Y., and Herrmann, H.: Size distributions of polycyclic aromatic hydrocarbons in urban atmosphere: Sorption mechanism and source contributions to respiratory deposition, Atmos. Chem. Phys., 16,

668 2971-2983, http://dx.doi.org/10.5194/acp-16-2971-2016, 2016.
669 Ma, W. L., Liu, L.Y., Jia, H. L., Yang, M., and Li, Y. F.: PAHs in Chinese atmosphere Part I:
670 Concentration, source and temperature dependence, Atmos. Environ., 173, 330-337,
671 https://doi.org/10.1016/j.atmosenv.2017.11.029, 2018.
672 Ma, W. L., Zhu, F. J., Hu, P. T., Qiao, L. N., and Li, Y. F.: Gas/particle partitioning of PAHs
673 based on equilibrium-state model and steady-state model, Sci. Total Environ., 706, 136029,
674 https://doi.org/10.1016/j.scitotenv.2019.136029, 2020.
675 Mastral, A. M., and Callén, M. S.: A review on polycyclic aromatic hydrocarbon (PAH)
676 emissions from energy generation, Environ. Sci. Technol., 34, 3051-3057,
677 https://doi.org/10.1021/es001028d, 2000.
678 Nisbet, I. C. T., and Lagoy, P. K.: Toxic equivalency factors (TEFs) for polycyclic aromatic
679 hydrocarbons (PAHs), Regul. Toxicol. Pharm., 16, 290-300, https://doi.org/10.1016/0273-
680 2300(92)90009-X, 1992.
681 Polissar, A. V., Hopke, P. K., and Paatero, P.: Atmospheric aerosol over Alaska-2. Elemental
682 composition and sources, J. Geophys. Res.-Atmos., 103, 19045-19057,
683 https://doi.org/10.1029/98jd01212, 1998.
684 Shen, H. Z., Huang, Y., Wang, R., Zhu, D., Li, W., Shen, G. F., Wang, B., Zhang, Y.Y., Chen, Y.
685 C., Lu, Y., Chen, H., Li, T. C., Sun, K., Li, B. G., Liu, W. X., Liu, J. F., and Tao, S.: Global
686 atmospheric emissions of polycyclic aromatic hydrocarbons from 1960 to 2008 and future
687 predictions, Environ. Sci. Technol., 47, 6415-6424, https://doi.org/10.1021/es400857z,
688 2013a.
689 Shen, G. F., Tao, S., Chen, Y. C., Zhang, Y. Y., Wei, S. Y., Xue, M., Wang, B., Wang, R., Lu, Y.,

690 Li, W., Shen, H. Z., Huang, Y., and Chen, H.: Emission characteristics for polycyclic
691 aromatic hydrocarbons from solid fuels burned in domestic stoves in rural China, Environ.
692 Sci. Technol., 47, 14485-14494, https://doi.org/10.1021/es403110b, 2013b.
693 Shen, R., Wang, Y., Gao, W., Cong, X., Cheng, L., and Li, X.: Size-segregated particulate matter
694 bound polycyclic aromatic hydrocarbons (PAHs) over China: Size distribution,
695 characteristics and health risk assessment, Sci. Total Environ., 685, 116-123,
696 https://doi.org/10.1016/j.scitotenv.2019.05.436, 2019.
697 Shrivastava, M., Lou, S., Zelenyuk, A., Easter, R. C., Corley, R. A., Thrall, B. D., Rasch, P. J.,
698 Fast, J. D., Massey Simonich, S.L., Shen, H., and Tao, S.: Global long-range transport and
699 lung cancer risk from polycyclic aromatic hydrocarbons shielded by coatings of organic
700 aerosol, P. Natl. Acad. Sci. USA, 114, 1246-1251,
701 https://doi.org/10.1073/pnas.1618475114, 2017.
702 Sofuoglu, A., Odabasi, M., Tasdemir, Y., Khalili, N. R., and Holsen, T. M.: Temperature
703 dependence of gas-phase polycyclic aromatic hydrocarbon and organochlorine pesticide
704 concentrations in Chicago air, Atmos. Environ., 35, 6503-6510,
705 https://doi.org/10.1016/S1352-2310(01)00408-3, 2001.
706 Song, C. B., He, J. J., Wu, L., Jin, T. S., Chen, X., Li, R. P., Ren, P. P., Zhang, L., and Mao, H.
707 J.: Health burden attributable to ambient $PM_{2.5}$ in China, Environ. Pollut., 223, 575-586,
708 http://dx.doi.org/10.1016/j.envpol.2017.01.060, 2017.
709 Sun, P., Blanchard, P., Brice, K. A., and Hites, R. A.: Trends in polycyclic aromatic hydrocarbon
710 concentrations in the Great Lakes atmosphere, Environ. Sci. Technol., 40, 6221-6227,
711 http://dx.doi.org/10.1021/es0607279, 2006.

712 Tan, J. H., Bi, X. H., Duan, J. C., Rahn, K. A., Sheng, G. Y., and Fu, J. M.: Seasonal variation
713 of particulate polycyclic aromatic hydrocarbons associated with PM_{10} in Guangzhou,
714 China, Atmos. Res., 80, 250-262, http://dx.doi.org/10.1016/j.atmosres.2005.09.004, 2006.
715 Tang, N., Suzuki, G., Morisaki, H., Tokuda, T., Yang, X. Y., Zhao, L. X., Lin, J. M., Kameda,
716 T., Toriba, A., and Hayakawa, K.: Atmospheric behaviors of particulate-bound polycyclic
717 aromatic hydrocarbons and nitropolycyclic aromatic hydrocarbons in Beijing, China from
718 2004 to 2010, Atmos. Environ., 152, 354-361,
719 http://dx.doi.org/10.1016/j.atmosenv.2016.12.056, 2017.
720 USEPA, 1991. Role of the baseline risk assessment in Superfund remedy-selection decisions.
721 Office of Solid Waste and Emergency Response, Washington.
722 Wang, G., Kawamura, K., Lee, S., Ho, K., and Cao, J.: Molecular, seasonal, and spatial
723 distributions of organic aerosols from fourteen Chinese cities, Environ. Sci. Technol., 40,
724 4619-4625, http://dx.doi.org/10.1021/es060291x, 2006.
725 Wang, G., Kawamura, K., Xie, M., Hu, S., Gao, S., Cao, J., An, Z., and Wang, Z.: Size-
726 distributions of n-alkanes, PAHs and hopanes and their sources in the urban, mountain and
727 marine atmospheres over East Asia, Atmos. Chem. Phys., 9, 8869-8882,
728 http://dx.doi.org/10.5194/acp-9-8869-2009, 2009.
729 Wang, Q. Y., Kobayashi, K., Lu, S. L., Nakajima, D., Wang, W. Q., Zhang, W. C., Sekiguchi,
730 K., and Terasaki, M.: Studies on size distribution and health risk of 37 species of polycyclic
731 aromatic hydrocarbons associated with fine particulate matter collected in the atmosphere
732 of a suburban area of Shanghai city, China, Environ. Pollut., 214, 149-160,
733 http://dx.doi.org/10.1016/j.envpol.2016.04.002, 2016.

734 Wang, W. T., Simonich, S. L. M., Wang, W., Giri, B., Zhao, J. Y., Xue, M., Cao, J., Lu, X. X.,
735 and Tao, S.: Atmospheric polycyclic aromatic hydrocarbon concentrations and gas/particle
736 partitioning at background, rural village and urban sites in the North China Plain, Atmos.
737 Res., 99, 197-206, http://dx.doi.org/10.1016/j.atmosres.2010.10.002, 2011.
738 World Health Organization (WHO), 2000. Air Quality Guidelines for Europe, 2nd Edition,
739 World Health Organization Regional Office for Europe, Copenhagen.
740 Xia, Z. H., Duan, X. L., Tao, S., Qiu, W. X., Liu, D., Wang, Y. L., Wei, S. Y., Wang, B., Jiang,
741 Q. J., Lu, B., Song, Y. X., and Hu, X. X.: Pollution level, inhalation exposure and lung
742 cancer risk of ambient atmospheric polycyclic aromatic hydrocarbons (PAHs) in Taiyuan,
743 China, Environ. Pollut., 173, 150-156, http://dx.doi.org/10.1016/j.envpol.2012.10.009,
744 2013.
745 Xu, H. J., Wang, X. M., Poesch, U., Feng, S. L., Wu, D., Yang, L., Li, S. X., Song, W., Sheng,
746 G. Y., and Fu, J. M.: Genotoxicity of total and fractionated extractable organic matter in
747 fine air particulate matter from urban Guangzhou: Comparison between haze and nonhaze
748 episodes, Environ. Toxicol. Chem., 27, 206-212, http://dx.doi.org/10.1897/07-095.1, 2008.
749 Xu, J., Chang, S. Y., Yuan, Z. H., Jiang, Y., Liu, S. N., Li, W. Z., and Ma, L. L.: Regionalized
750 techno-economic assessment and policy analysis for biomass molded fuel in China,
751 Energies, 8, 13846-13863, http://dx.doi.org/10.3390/en81212399, 2015.
752 Xu, S. S., Liu, W. X., and Tao, S.: Emission of polycyclic aromatic hydrocarbons in China,
753 Environ. Sci. Technol., 40, 702-708, http://dx.doi.org/10.1021/es0517062, 2006.
754 Xue, Y. F., Zhou, Z., Nie, T., Wang, K., Nie, L., Pan, T., Wu, X. Q., Tian, H. Z., Zhong, L. H.,
755 Li, J., Liu, H. J., Liu, S. H., and Shao, P.Y.: Trends of multiple air pollutants emissions

from residential coal combustion in Beijing and its implication on improving air quality for control measures, Atmos. Environ., 142, 303-312, http://dx.doi.org/10.1016/j.atmosenv.2016.08.004, 2016.

Yang, G. H., Wang, Y., Zeng, Y. X., Gao, G. F., Liang, X. F., Zhou, M. G., Wan, X., Yu, S. C., Jiang, Y. H., Naghavi, M., Vos, T., Wang, H. D., Lopez, A. D., and Murray, C. J. L.: Rapid health transition in China, 1990-2010: Findings from the Global Burden of Disease Study 2010, Lancet, 381, 1987-2015, http://dx.doi.org/10.1016/S0140-6736(13)61097-1, 2013.

Yang, Y. Y., Guo, P. R., Zhang, Q., Li, D. L., Zhao, L., and Mu, D. H.: Seasonal variation, sources and gas/particle partitioning of polycyclic aromatic hydrocarbons in Guangzhou, China, Sci. Total Environ., 408, 2492-2500, http://dx.doi.org/10.1016/j.scitotenv.2010.02.043, 2010.

Yin, P., Guo, J., Wang, L., Fan, W., Lu, F., Guo, M., Moreno, S.B.R., Wang, Y., Wang, H., Zhou, M., and Dong, Z.: Higher risk of cardiovascular disease associated with smaller size-fractioned particulate matter, Environ. Sci. Technol. Let., 7, 95-101, https://dx.doi.org/10.1021/acs.estlett.9b00735, 2020.

Yu, Q. Q., Gao, B., Li, G. H., Zhang, Y. L., He, Q. F., Deng, W., Huang, Z. H., Ding, X., Hu, Q. H., Huang, Z. Z., Wang, Y. J., Bi, X. H., and Wang, X. M.: Attributing risk burden of $PM_{2.5}$-bound polycyclic aromatic hydrocarbons to major emission sources: Case study in Guangzhou, south China, Atmos. Environ., 142, 313-323, http://dx.doi.org/10.1016/j.atmosenv.2016.08.009, 2016.

Yu, Q. Q., Yang, W. Q., Zhu, M., Gao, B., Li, S., Li, G. H., Fang, H., Zhou, H. S., Zhang, H. N., Wu, Z. F., Song, W., Tan, J. H., Zhang, Y. L., Bi, X. H., Chen, L. G., and Wang, X. M.:

778 Ambient $PM_{2.5}$-bound polycyclic aromatic hydrocarbons (PAHs) in rural Beijing:
779 Unabated with enhanced temporary emission control during the 2014 APEC summit and
780 largely aggravated after the start of wintertime heating, Environ. Pollut., 238, 532-542,
781 https://doi.org/10.1016/j.envpol.2018.03.079, 2018.
782 Yu, Y. X., Li, Q., Wang, H., Wang, B., Wang, X.L., Ren, A. G., and Tao, S.: Risk of human
783 exposure to polycyclic aromatic hydrocarbons: A case study in Beijing, China, Environ.
784 Pollut., 205, 70-77, http://dx.doi.org/10.1016/j.envpol.2015.05.022, 2015.
785 Yunker, M. B., Macdonald, R. W., Vingarzan, R., Mitchell, R. H., Goyette, D., and Sylvestre,
786 S.: PAHs in the Fraser River basin: A critical appraisal of PAH ratios as indicators of PAH
787 source and composition, Org. Geochem., 33, 489-515, http://dx.doi.org/10.1016/S0146-
788 6380(02)00002-5, 2002.
789 Zelenyuk, A., Imre, D., Beranek, J., Abramson, E., Wilson, J., and Shrivastava, M.: Synergy
790 between secondary organic aerosols and long-range transport of polycyclic aromatic
791 hydrocarbons, Environ. Sci. Technol., 46, 12459-12466,
792 http://dx.doi.org/10.1021/es302743z, 2012.
793 Zhang, K., Zhang, B. Z., Li, S. M., Wong, C. S., and Zeng, E. Y.: Calculated respiratory
794 exposure to indoor size-fractioned polycyclic aromatic hydrocarbons in an urban
795 environment, Sci. Total Environ., 431, 245-251,
796 http://dx.doi.org/10.1016/j.scitotenv.2012.05.059, 2012.
797 Zhang, Y. S., Shao, M., Lin, Y., Luan, S. J., Mao, N., Chen, W. T., and Wang, M.: Emission
798 inventory of carbonaceous pollutants from biomass burning in the Pearl River Delta
799 Region, China, Atmos. Environ., 76, 189-199,

800 http://dx.doi.org/10.1016/j.atmosenv.2012.05.055, 2013.
801 Zhang, X. L., Tao, S., Liu, W. X., Yang, Y., Zuo, Q., and Liu, S. Z.: Source diagnostics of
802 polycyclic aromatic hydrocarbons based on species ratios: A multimedia approach,
803 Environ. Sci. Technol., 39, 9109-9114, http://dx.doi.org/10.1021/es0513741, 2005.
804 Zhang, Y. X., and Tao, S.: Seasonal variation of polycyclic aromatic hydrocarbons (PAHs)
805 emissions in China, Environ. Pollut., 156, 657-663,
806 http://dx.doi.org/10.1016/j.envpol.2008.06.017, 2008.
807 Zhang, Y. X., and Tao, S.: Global atmospheric emission inventory of polycyclic aromatic
808 hydrocarbons (PAHs) for 2004, Atmos. Environ., 43, 812-819,
809 http://dx.doi.org/10.1016/j.atmosenv.2008.10.050, 2009.
810 Zhang, Y. X., Tao, S., Cao, J., and Coveney, R. M.: Emission of polycyclic aromatic
811 hydrocarbons in China by county, Environ. Sci. Technol., 41, 683-687,
812 http://dx.doi.org/10.1021/es061545h, 2007.
813 Zhang, Y., Shen, H., Tao, S., and Ma, J.: Modeling the atmospheric transport and outflow of
814 polycyclic aromatic hydrocarbons emitted from China, Atmos. Environ., 45, 2820-2827,
815 http://dx.doi.org/10.1016/j.atmosenv.2011.03.006, 2011.
816 Zhang, Y. X., Tao, S., Shen, H. Z., and Ma, J. M.: Inhalation exposure to ambient polycyclic
817 aromatic hydrocarbons and lung cancer risk of Chinese population, P. Natl. Acad. Sci.
818 USA, 106, 21063-21067, http://dx.doi.org/10.1073/pnas.0905756106, 2009.
819 Zhu, L. Z., Lu, H., Chen, S. G., and Amagai, T.: Pollution level, phase distribution and source
820 analysis of polycyclic aromatic hydrocarbons in residential air in Hangzhou, China, J.
821 Hazard. Mater., 162, 1165-1170, http://dx.doi.org/10.1016/j.jhazmat.2008.05.150, 2009.

822 Zhu, Y., Tao, S., Price, O. R., Shen, H. Z., Jones, K. C., and Sweetman, A. J.: Environmental
823 distributions of benzo[a]pyrene in China: Current and future emission reduction scenarios
824 explored using a spatially explicit multimedia fate model, Environ. Sci. Technol., 49,
825 13868-13877, http://dx.doi.org/10.1021/acs.est.5b00474, 2015.

826

827

828 Table 1 PAHs concentration measured in this study and comparison with those of other large scale
829 observations.

Site/type	Sampling period	Sample type	# of sites	# of species	PAHs (ng/m^3)	Reference
China[a]	Oct, 2012-Sep, 2013	$PM_{1.1}$	12	24	3.4-126.2	This study
China[a]	Oct, 2012-Sep, 2013	$PM_{1.1\text{-}3.3}$	12	24	2.4-55.7	This study
China[a]	Oct, 2012-Sep, 2013	$PM_{>3.3}$	12	24	1.8-22.7	This study
China/Urban	2003	$PM_{2.5}$	14	18	1.7-701	Wang et al., 2006
China[b]	2005	PUF	40	20	374.5[e]	Liu et al., 2007
China/Urban	2013-2014	$PM_{2.5}$	9	16	14-210	Liu et al., 2017b
China/Urban	Aug, 2008-July, 2009	$PM_{2.5}$	11	16	75.4-478	Ma et al., 2018
China[c]	Jan, 2013-Dec, 2014	$PM_{9.0}$[e]	10	12	17.3-244.3	Shen et al., 2019
Great Lakes	1996-2003	PUF	7	16	0.59-70	Sun et al., 2006
Asian countries[d]	Sep, 2012-Aug, 2013	PUF	176	47	6.29-688	Hong et al., 2016
U.S.	1990-2014	PUF	169	15	52.6	Liu et al., 2017a
Japan	1997-2014	TSP	5	9	0.21-3.73	Hayakawa et al., 2018
Europe	2002	PUF	22	12	0.5-61.2	Jaward et al., 2004

830 a: including 5 urban sites, 3 sub-urban sites and 4 remote sites in China
831 b: including 37 cities and 3 rural locations in China
832 c: including 5 urban sites, 1 sub-urban site, 1 farmland site and 3 background sites in China
833 d: including 82 urban sites, 83 rural sites and 11 background sites in China, Japan, South Korea,
834 Vietnam, and India
835 e: the unit was ng/day
836

837 Table 2 Correlation coefficient (r), significance (p) of PAHs between paired sites in each region.

	Northern China			Southern China	
regions	north	northeast	northwest	east	southwest
paired sites	BJ-TY	HL-TYU	DH-SPT	WX-HF	KM-BN
distance between sites	400 km	450 km	940 km	280 km	380 km
r	0.97	0.80	0.63	0.77	-
p	<0.001	<0.001	0.001	<0.001	0.09

838

839

840

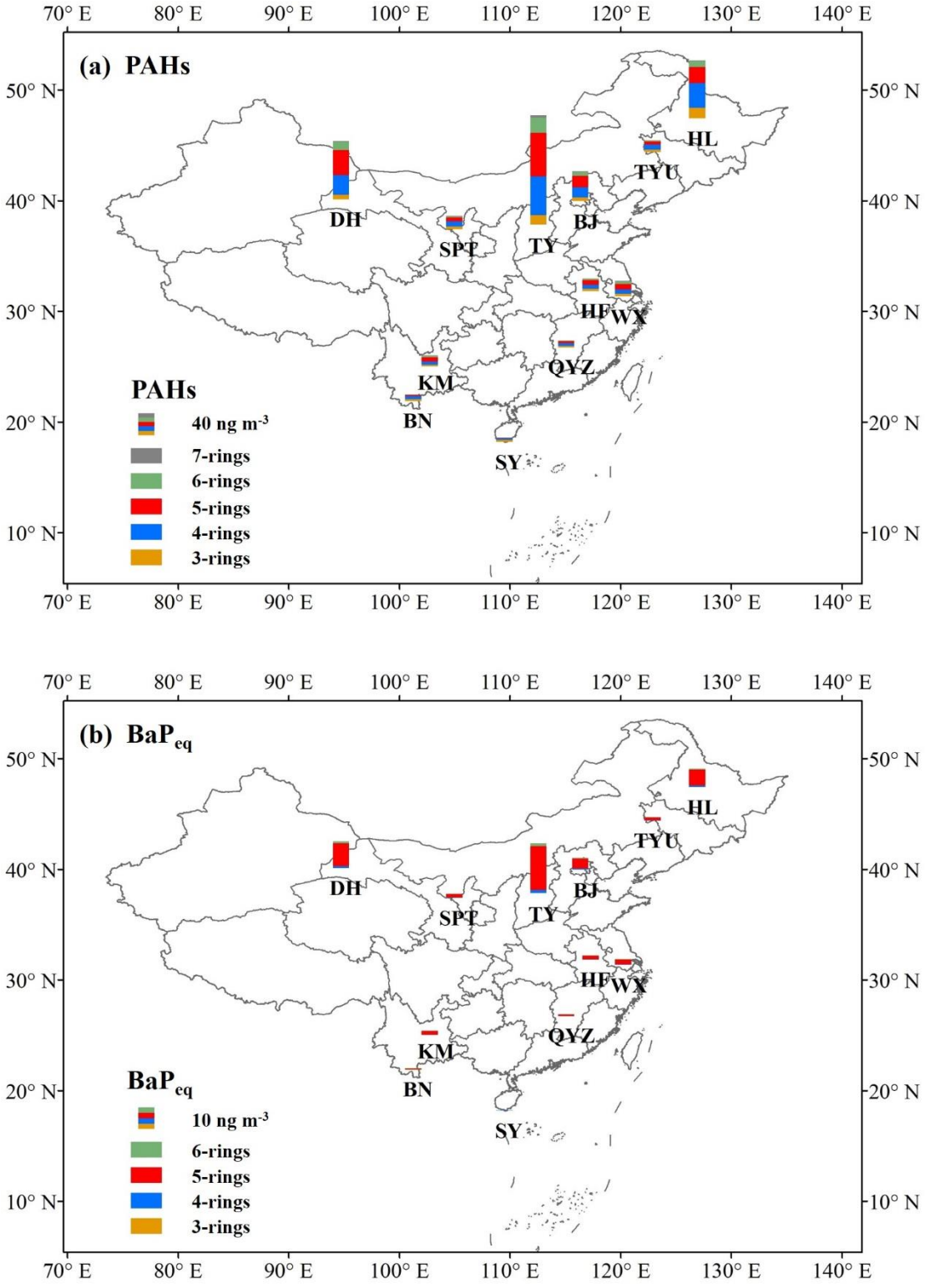

841

842 Figure 1 Annual averages of $\sum_{24}$PAHs (a) and BaP_{eq} (b) at 12 sites in China.

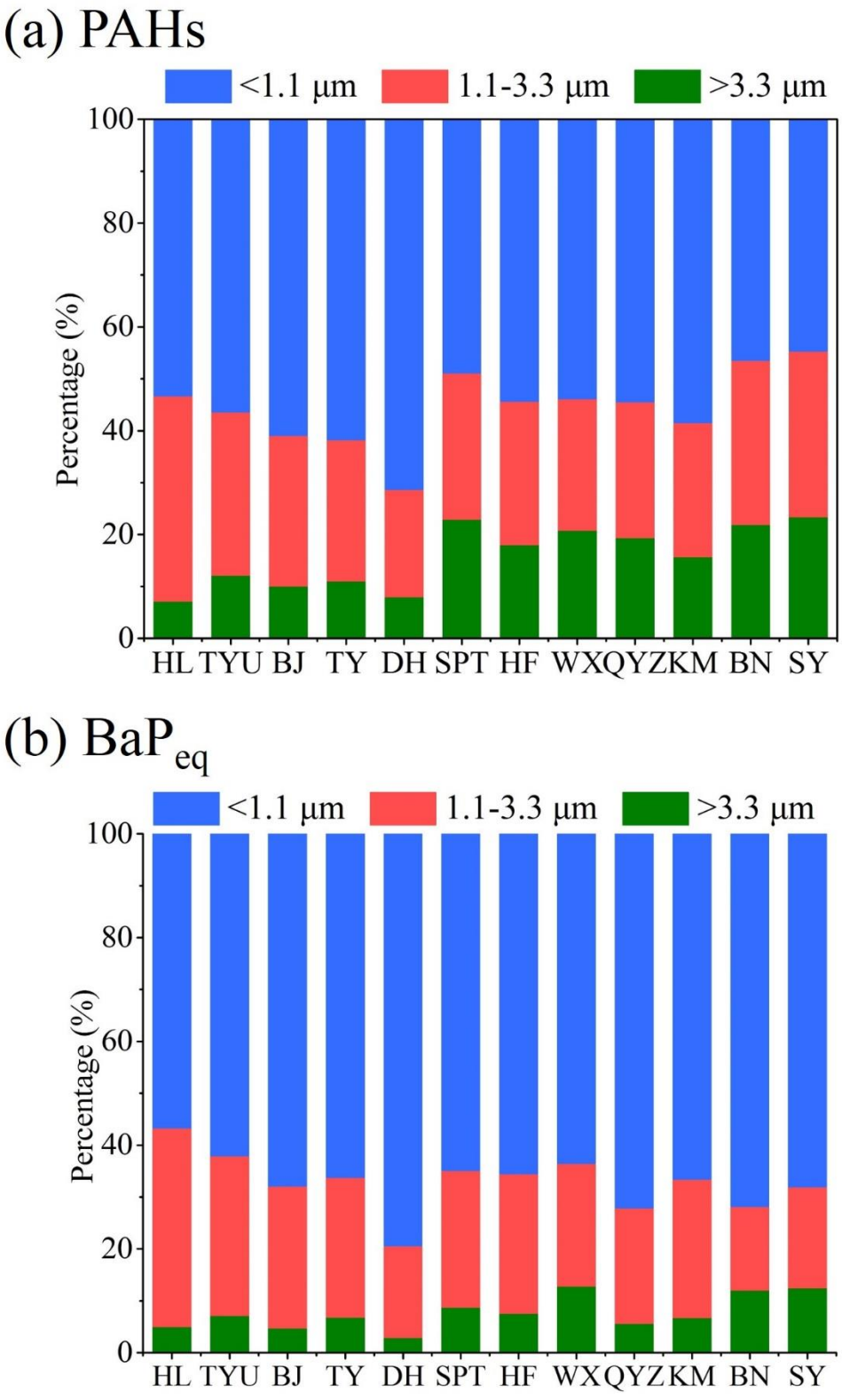

Figure 2 Size distribution of total measured PAHs (a) and BaP_{eq} (b) at 12 sites over China.

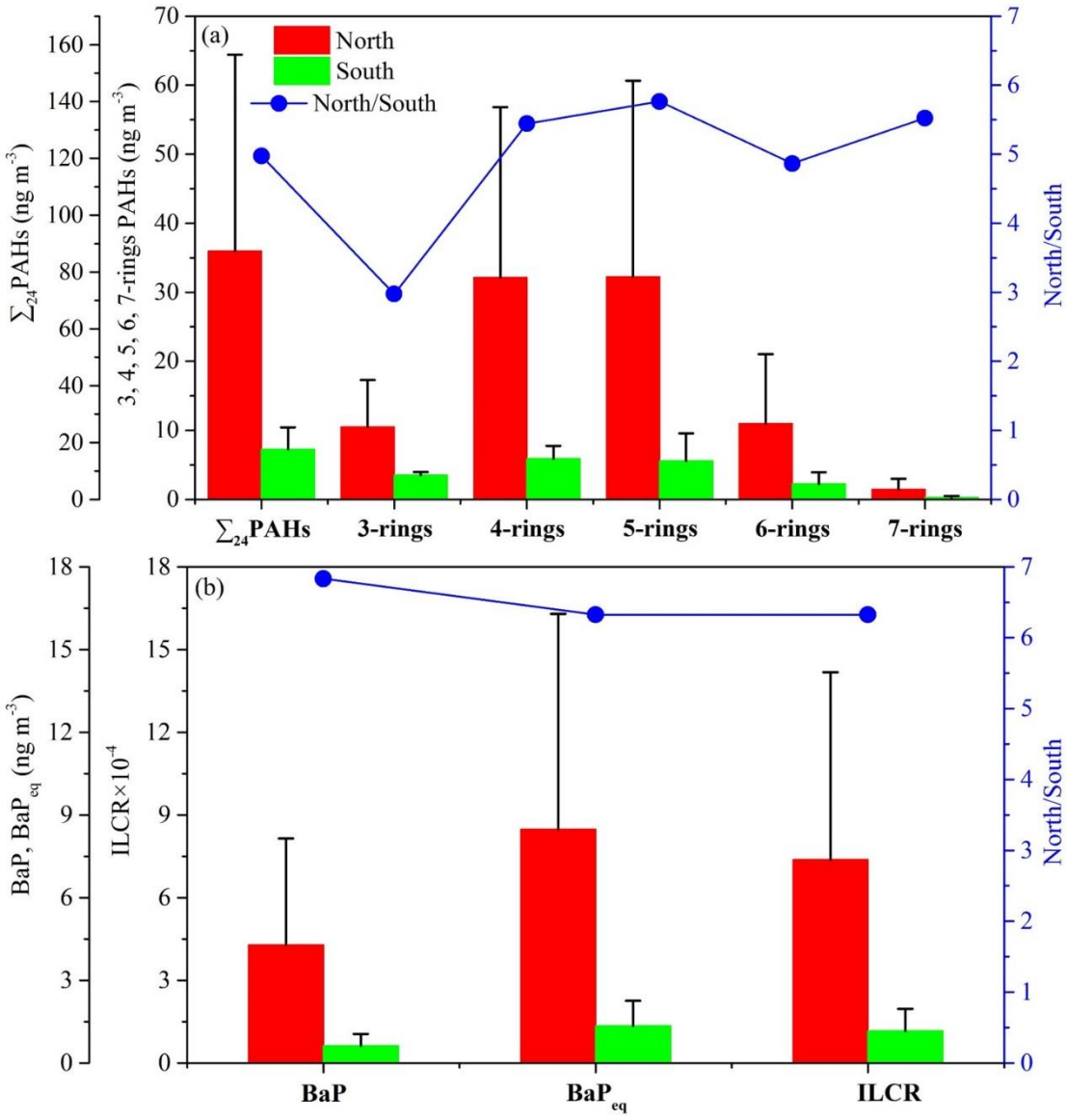

846

847 Figure 3 Comparison between the northern and the southern China in $\sum_{24}$PAHs, 3-7 rings PAHs

848 (a) and BaP, BaP$_{eq}$ and ILCR (b).

849

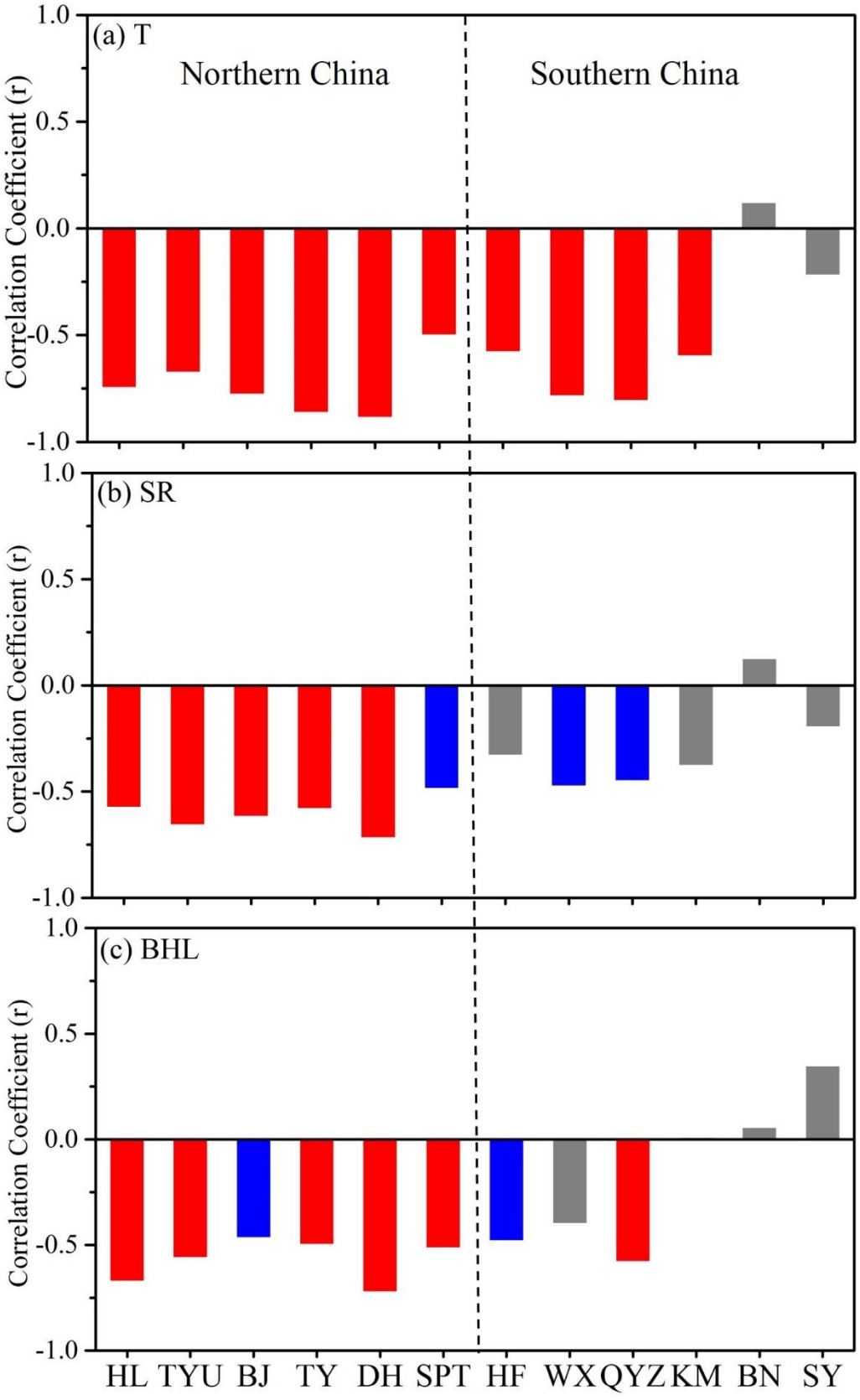

850

851 Figure 4 Correlation coefficient (r) of PAHs with T (a), SR (b) and BLH (c) at 12 sites. The

852 red, blue and gray bars indicate $p<0.01$, $p<0.05$ and $p>0.05$, respectively.

853

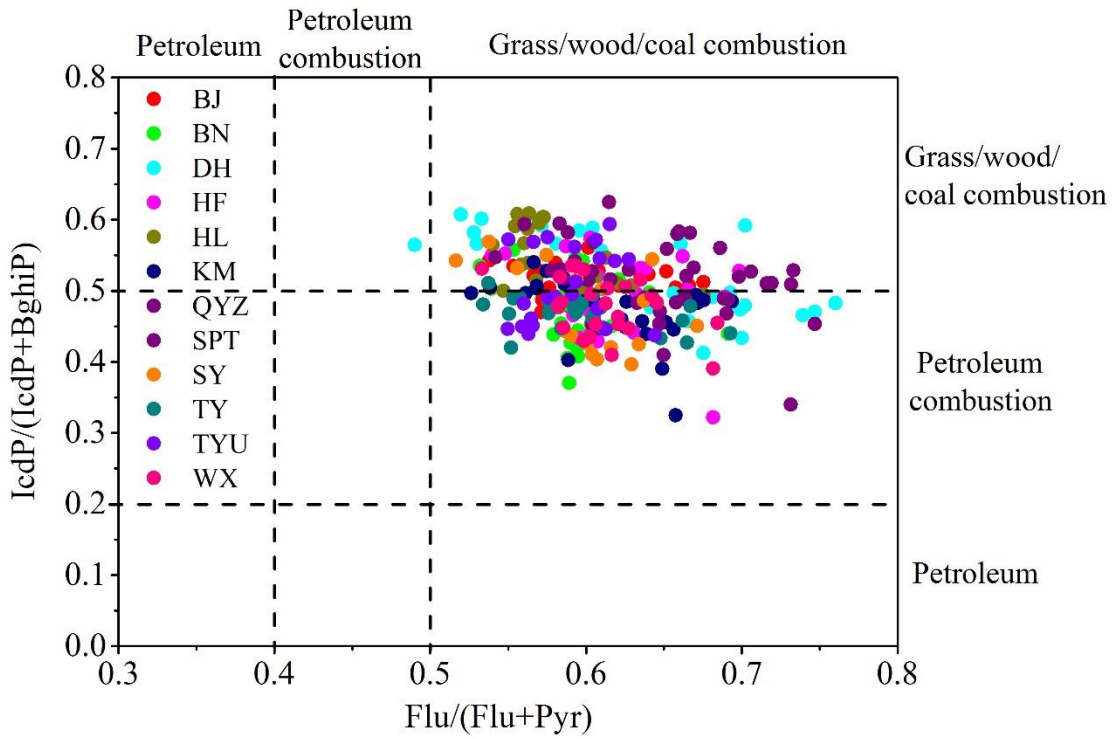

854

855 Figure 5 Diagnostic ratios of IcdP/(IcdP +BgiP) versus Flu/(Flu+Pyr) at 12 sites in China.

856 Ranges of ratios for sources are adopted from Yunker et al. (2002).

857

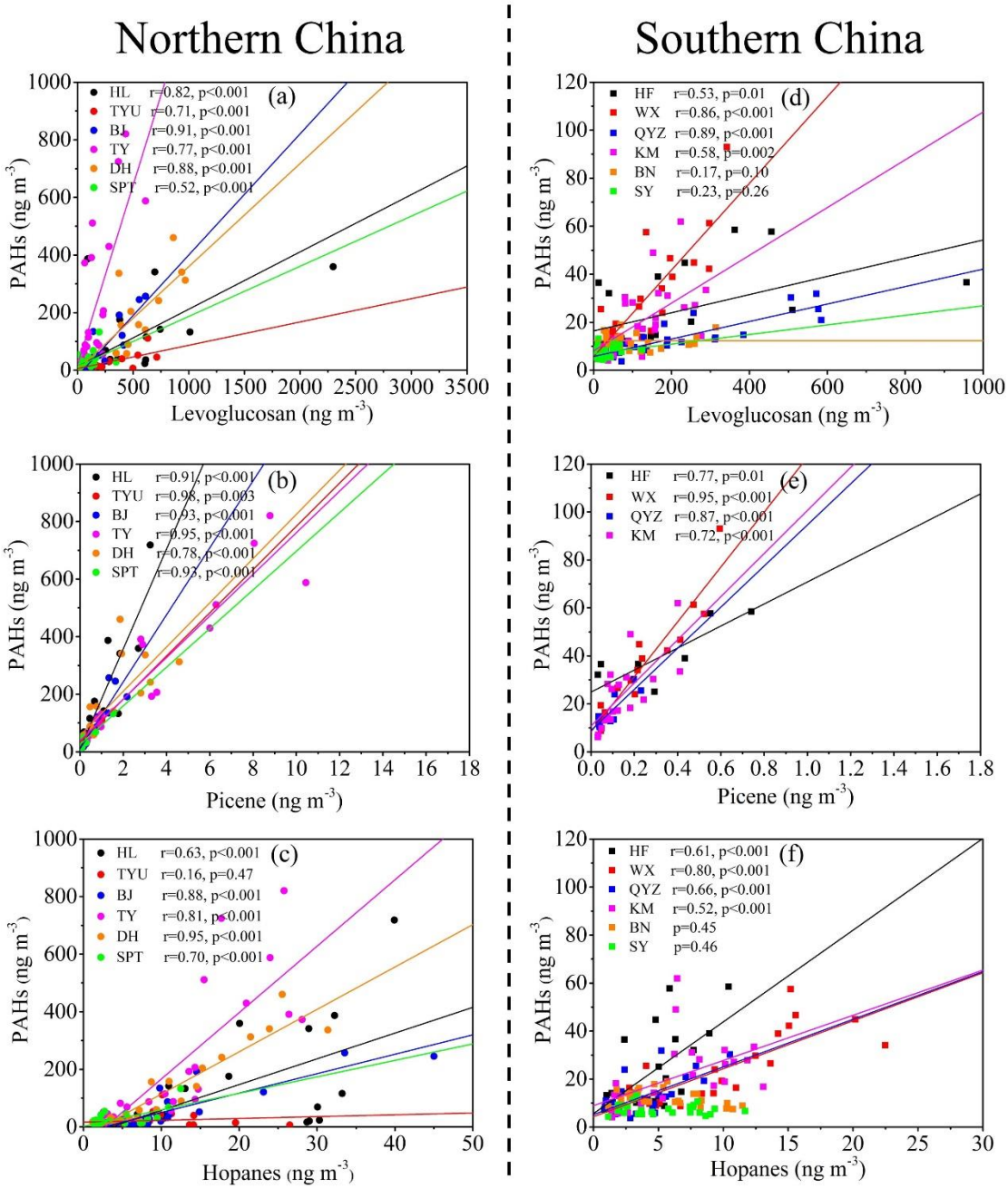

858

859 Figure 6 The correlation between PAHs and levoglucosan, picene and hopanes at sites in the

860 northern China (a-c) and the southern China (d-f).

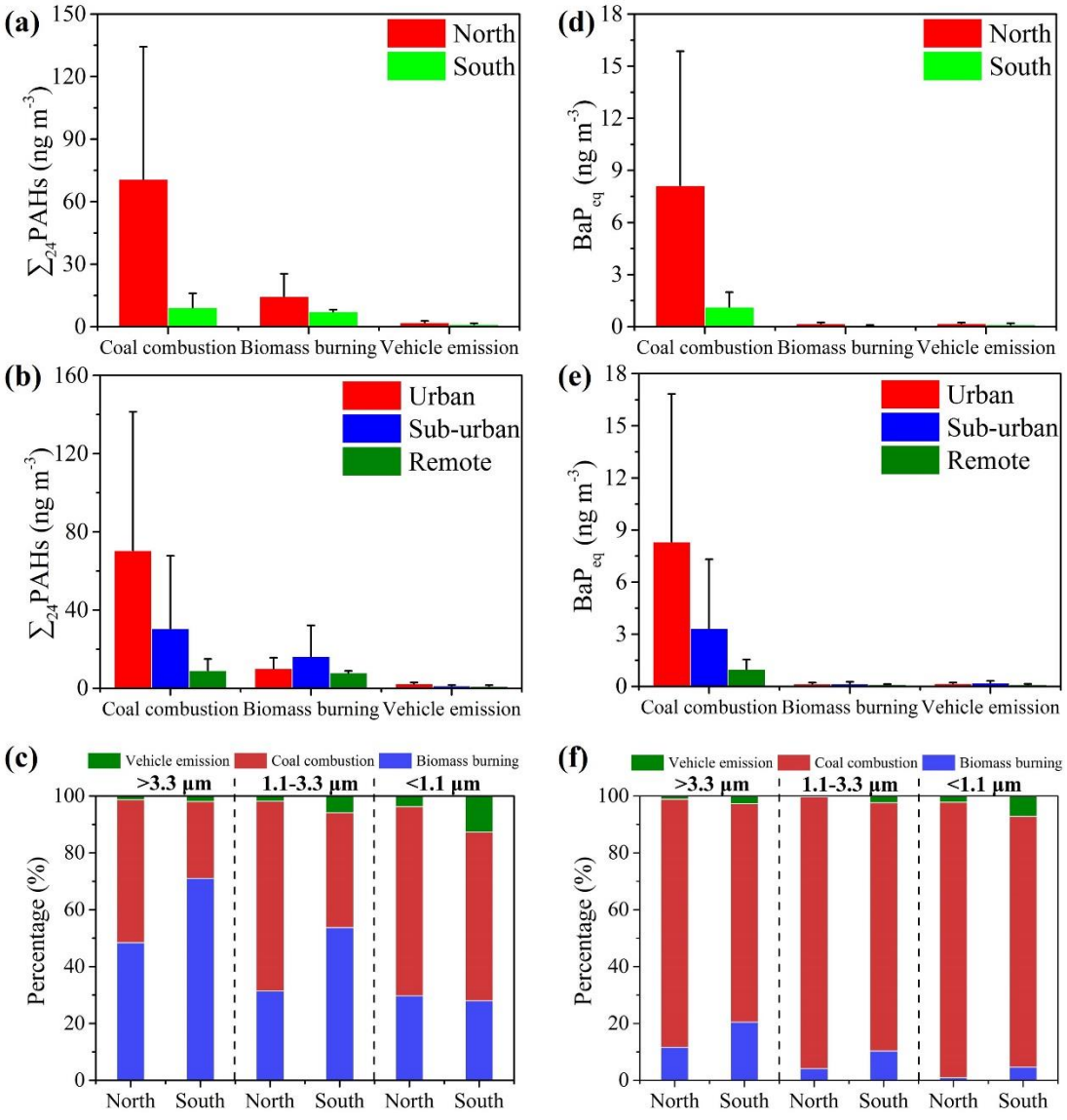

861

862 Figure 7 Source apportionment of $\sum_{24}$ PAHs and BaP_{eq} in different regions (a, d), sampling sites

863 (b, e) and size particles (c, f).

864

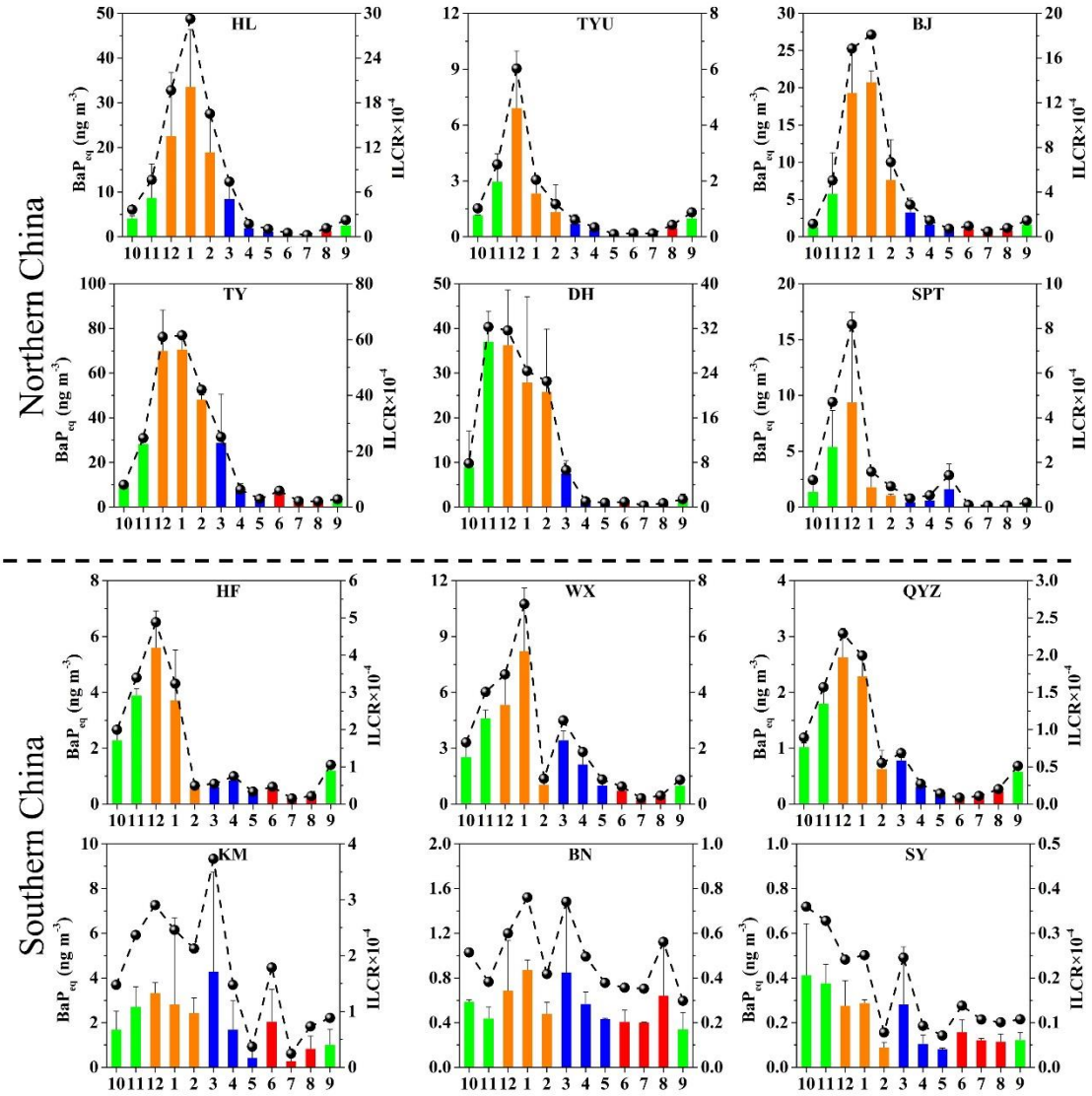

Figure 8 Monthly variations of BaP_{eq} and ILCR at sites in the northern China and the southern China. The green, yellow, blue and red bars represent BaP_{eq} in fall (October − November, 2012 and September, 2013), winter (December 2012 – February 2013), spring (March – May, 2013), and summer (June − August, 2013), respectively.

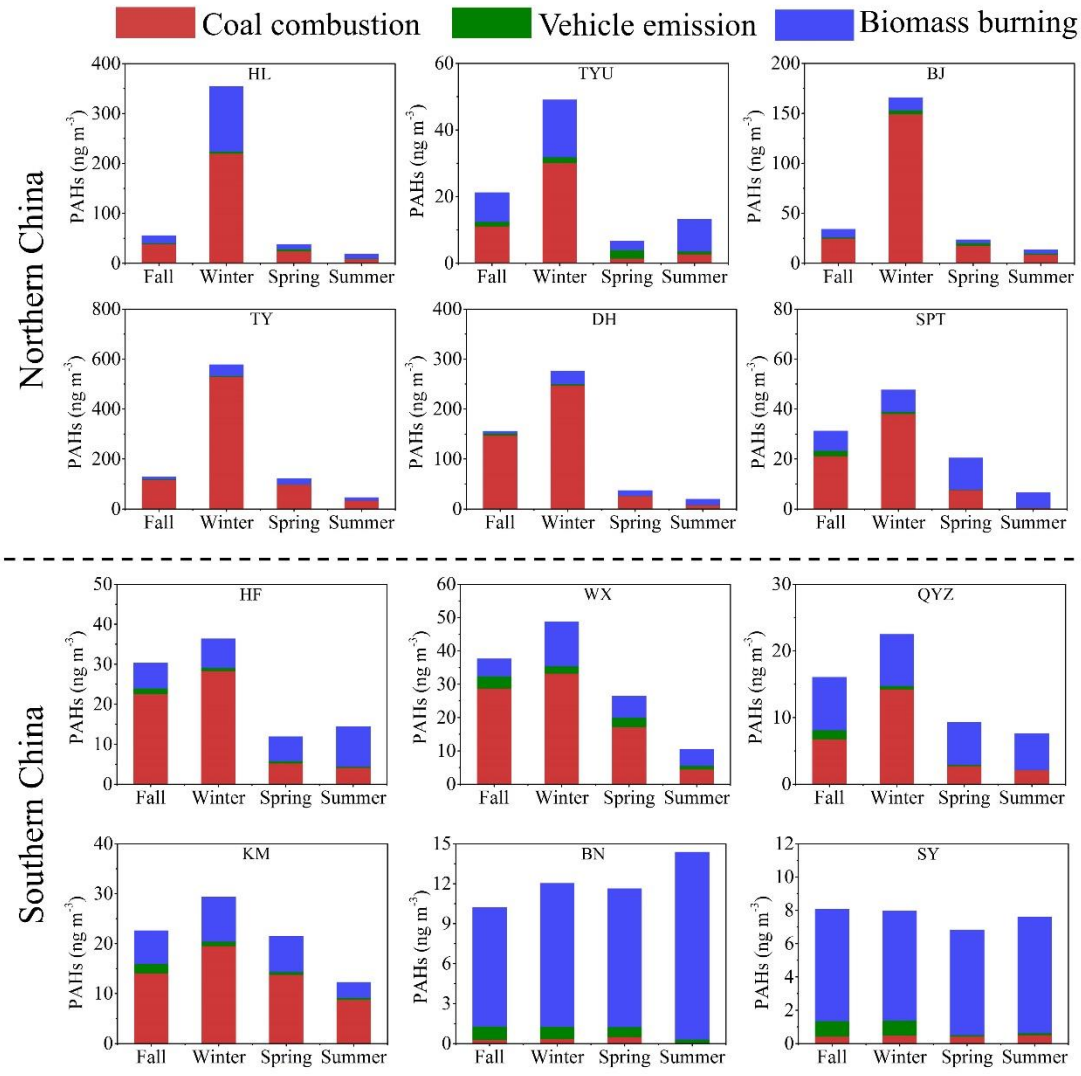

Figure 9 Seasonal variations of PAHs source contributions in China.